

Evaluating the Gapless Color-Flavor Locked Phase

Mark Alford

Physics Department, Washington University, St. Louis, MO 63130, USA

Chris Kouvaris and Krishna Rajagopal

Center for Theoretical Physics, Massachusetts Institute of Technology, Cambridge, MA 02139, USA

(Dated: June 11, 2004)

In neutral cold quark matter that is sufficiently dense that the strange quark mass M_s is unimportant, all nine quarks (three colors; three flavors) pair in a color-flavor locked (CFL) pattern, and all fermionic quasiparticles have a gap. We recently argued that the next phase down in density (as a function of decreasing quark chemical potential μ or increasing strange quark mass M_s) is the new “gapless CFL” (“gCFL”) phase in which only seven quasiparticles have a gap, while there are gapless quasiparticles described by two dispersion relations at three momenta. There is a continuous quantum phase transition from CFL to gCFL quark matter at $M_s^2/\mu \approx 2\Delta$, with Δ the gap parameter. Gapless CFL, like CFL, leaves unbroken a linear combination \tilde{Q} of electric and color charges, but it is a \tilde{Q} -conductor with gapless \tilde{Q} -charged quasiparticles and a nonzero electron density. In this paper, we evaluate the gapless CFL phase, in several senses. We present the details underlying our earlier work which showed how this phase arises. We display all nine quasiparticle dispersion relations in full detail. Using a general pairing ansatz that only neglects effects that are known to be small, we perform a comparison of the free energies of the gCFL, CFL, 2SC, gapless 2SC, and 2SCus phases. We conclude that as density drops, making the CFL phase less favored, the gCFL phase is the next spatially uniform quark matter phase to occur. A mixed phase made of colored components would have lower free energy if color were a global symmetry, but in QCD such a mixed phase is penalized severely.

PACS numbers:

I. INTRODUCTION

Because QCD is asymptotically free, we expect that matter at sufficiently high densities and/or temperatures will consist of almost-free quarks and gluons. However, over the last few years it has become clear that there is a rich and varied landscape of phases lying between these asymptotic regimes and the familiar hadronic phase at low temperature and density. In the region where the temperature is low and the density is high enough that hadrons are crushed into quark matter, there is a whole family of “color superconducting” phases [1]. The essence of color superconductivity is quark pairing, driven by the BCS mechanism, which operates when there exists an attractive interaction between fermions at a Fermi surface. The QCD quark-quark interaction is strong, and is attractive in many channels, so we expect cold dense quark matter to *generically* exhibit color superconductivity. Moreover, quarks, unlike electrons, have color and flavor as well as spin degrees of freedom, so many different patterns of pairing are possible. This leads us to expect a rich phase structure in matter beyond nuclear density.

Color superconducting quark matter may well occur naturally in the universe, in the cold dense cores of compact (“neutron”) stars, where densities are above nuclear density, and temperatures are of the order of tens of keV. In future low-energy heavy ion colliders, such as the Compressed Baryonic Matter Experiment at the future accelerator facility at GSI Darmstadt [2], it could conceivably be possible to create color superconducting quark matter

(or perhaps hot dense matter that is in the quark-gluon plasma phase but which exhibits fluctuations that are precursors of color superconductivity [3]).

It is by now well-established that at asymptotic densities, where the up, down and strange quarks can be treated on an equal footing and the potentially disruptive strange quark mass can be neglected, quark matter is in the color-flavor locked (CFL) phase, in which quarks of all three colors and all three flavors form Cooper pairs [4]. However, just as RHIC is teaching us about the properties of the hot but far from asymptotically hot quark-gluon plasma [5], we should expect that if neutron star cores are made of color superconducting quark matter, they may not reach the densities at which CFL predominates. In this paper, as in Ref. [6], we ask what form of color superconducting quark matter is the “next phase down in density”. That is, we imagine beginning in the CFL phase at asymptotic density, reducing the density, and assume that CFL pairing is disrupted by the heaviness of the strange quark before color superconducting quark matter is superseded by the hadronic phase. Upon making this assumption, we ask what form the disruption takes and what are the properties of the resulting phase of dense, but not asymptotically dense, matter.

To describe quark matter as may exist in the cores of compact stars, we consider quark chemical potentials μ of order 500 MeV at most. The strange quark mass M_s must then be included: it is expected to be density dependent, lying between the current mass ~ 100 MeV and the vacuum constituent quark mass ~ 500 MeV. In bulk matter, as is relevant for compact stars where we are

interested in kilometer-scale volumes, we must furthermore require electromagnetic and color neutrality [7, 8] (possibly via mixing of oppositely-charged phases) and allow for equilibration under the weak interaction. All these factors work to pull apart the Fermi momenta of the different quark species, imposing an energy cost on the cross-species pairing that characterizes color-flavor locking. At the highest densities we expect CFL pairing, but as the density decreases the combination of nonzero M_s and the constraints of neutrality put greater and greater stress on cross-species pairing, and we expect transitions to other pairing patterns.

In this paper we study the first of these transitions, and work exclusively at zero temperature, which is a reasonable approximation in the interior of a neutron star that is more than a few seconds old. (Nonzero temperature adds interesting new facets to the analysis [9], that we shall further analyze elsewhere.) We argue that the CFL phase will first give way, via a continuous phase transition, to a new phase with gapless fermions that we call gapless CFL (gCFL). The transition occurs when $M_s^2/\mu \simeq 2\Delta$, where Δ is the pairing gap parameter. The gCFL phase has gapless modes and nonzero electron density. Although it has the same symmetries as the CFL phase, gapless CFL matter is a conductor whereas CFL quark matter is a dielectric insulator.

A. Summary of the CFL phase

To set the stage for our analysis, we briefly summarize the properties of the CFL phase [4]. If we set all three quark masses to zero, the diquark condensate in the CFL phase spontaneously breaks the full symmetry group of QCD,

$$\begin{aligned} [SU(3)_{\text{color}}] \times \underbrace{SU(3)_L \times SU(3)_R \times U(1)_B}_{\supset [U(1)_Q]} \\ \rightarrow \underbrace{SU(3)_{C+L+R}}_{\supset [U(1)_{\tilde{Q}}]} \times \mathbb{Z}_2 \end{aligned} \quad (1)$$

where $SU(3)_{\text{color}}$ and electromagnetism $U(1)_Q$ are gauged, and the unbroken $SU(3)_{C+L+R}$ subgroup consists of flavor rotations of the left and right quarks with equal and opposite color rotations, and contains an unbroken gauged “rotated electromagnetism” $U(1)_{\tilde{Q}}$ [4, 10]. The CFL phase has the largest possible unbroken symmetry consistent with diquark condensation, achieved by having all nine quarks participate equally in the pairing, and this gives the maximal pairing free energy benefit. Not surprisingly, *ab initio* calculations valid at asymptotic densities confirm that the CFL phase is the ground state of QCD in the high density limit [1, 11].

In the limit of three massless quarks described above there are 17 broken symmetry generators in the CFL phase, 8 of which become longitudinal components of

massive gauge bosons and 9 of which remain as Goldstone bosons. However, in the real world there are two light quark flavors, the up (u) and down (d), with masses $\lesssim 10$ MeV, and a medium-weight flavor, the strange (s) quark, with mass $\gtrsim 100$ MeV. The strange quark therefore plays a crucial role in the phases of QCD. In the presence of quark masses, the eight Goldstone bosons coming from the breaking of chiral symmetries acquire masses [1, 4, 12], and furthermore the CFL condensate may rotate within the manifold describing these mesons [13]. In analyzing the response of the CFL phase to the strange quark mass, we shall be concerned with the dispersion relations describing its fermionic quasiparticles, as they signal an instability corresponding to the disruption of pairing itself. In this analysis, we shall neglect flavor rotations of the CFL condensate, as the direct effects of such meson condensates on the stability or instability with respect to pair breaking is minimal. (Meson condensates would play an important indirect role if they were charged, but the favored meson condensation channels are neutral assuming that the neutrino density is negligible [13].) The ninth Goldstone boson, that corresponding to the spontaneous breaking of $U(1)_B$ and hence to superfluidity, remains massless even once quark masses are taken into account and therefore plays a crucial role in many low energy properties of the CFL phase, for example in its viscosity [14], specific heat, neutrino opacity, and neutrino emissivity at low temperatures [15].

B. (Gapless) CFL Pairing Ansatz

To study the response of the CFL phase to a non-negligible strange quark mass, we use the pairing ansatz [4]

$$\langle \psi_a^\alpha C \gamma_5 \psi_b^\beta \rangle \sim \Delta_1 \epsilon^{\alpha\beta 1} \epsilon_{ab1} + \Delta_2 \epsilon^{\alpha\beta 2} \epsilon_{ab2} + \Delta_3 \epsilon^{\alpha\beta 3} \epsilon_{ab3} \quad (2)$$

Here ψ_a^α is a quark of color $\alpha = (r, g, b)$ and flavor $a = (u, d, s)$; the condensate is a Lorentz scalar, antisymmetric in Dirac indices, antisymmetric in color (the channel with the strongest attraction between quarks), and consequently antisymmetric in flavor. The gap parameters Δ_1 , Δ_2 and Δ_3 describe down-strange, up-strange and up-down Cooper pairs, respectively. They describe a 9×9 matrix in color-flavor space that, in the basis $(ru, gd, bs, rd, gu, rs, bu, gs, bd)$, takes the form

$$\Delta = \begin{pmatrix} 0 & \Delta_3 & \Delta_2 & 0 & 0 & 0 & 0 & 0 & 0 \\ \Delta_3 & 0 & \Delta_1 & 0 & 0 & 0 & 0 & 0 & 0 \\ \Delta_2 & \Delta_1 & 0 & 0 & 0 & 0 & 0 & 0 & 0 \\ 0 & 0 & 0 & 0 & -\Delta_3 & 0 & 0 & 0 & 0 \\ 0 & 0 & 0 & -\Delta_3 & 0 & 0 & 0 & 0 & 0 \\ 0 & 0 & 0 & 0 & 0 & 0 & -\Delta_2 & 0 & 0 \\ 0 & 0 & 0 & 0 & 0 & -\Delta_2 & 0 & 0 & 0 \\ 0 & 0 & 0 & 0 & 0 & 0 & 0 & 0 & -\Delta_1 \\ 0 & 0 & 0 & 0 & 0 & 0 & 0 & -\Delta_1 & 0 \end{pmatrix} \quad (3)$$

We see that (rd, gu) , (bu, rs) and (gs, bd) quarks pair with gap parameters Δ_1 , Δ_2 and Δ_3 respectively, while the (ru, gd, bs) quarks pair among each other involving all the Δ 's. The most important physics that we are leaving out by making this ansatz is pairing in which the Cooper pairs are symmetric in color, and therefore also in flavor. Diquark condensates of this form break no new symmetries, and therefore *must* arise in the CFL phase [4, 16]. However because the QCD interaction is repulsive between quarks that are symmetric in color these condensates are numerically insignificant [4, 9, 16]. To find which phases occur in realistic quark matter, we must take into account the strange quark mass and equilibration under the weak interaction, and impose neutrality under the color and electromagnetic gauge symmetries. The arguments that favor (2) are unaffected by these considerations, but there is no reason for the gap parameters to be equal once $M_s \neq 0$. Much previous work [8, 16, 17, 18, 19, 20] compared color-flavor-locked (CFL) phase (favored in the limit $M_s \rightarrow 0$ or $\mu \rightarrow \infty$), the two-flavor (2SC) phase (favored in the limit $M_s \rightarrow \infty$), and unpaired quark matter. We gave a model-independent argument in Ref. [6], however, that when the CFL phase is disrupted, it cannot give way to either 2SC or unpaired quark matter. Above a critical M_s^2/μ , we found that the CFL phase is replaced by a new gapless CFL (gCFL) phase, not by 2SC quark matter. The defining (and eponymous) properties of the gapless CFL phase arise in its dispersion relations, not in its pattern of gap parameters. However, it is useful for orientation to list the patterns of gap parameters for all the phases we shall discuss:

$$\Delta_3 \simeq \Delta_2 = \Delta_1 = \Delta_{CFL} \quad \text{CFL} \quad (4)$$

$$\Delta_3 > 0, \quad \Delta_1 = \Delta_2 = 0 \quad \text{(gapless) 2SC} \quad (5)$$

$$\Delta_2 > 0, \quad \Delta_1 = \Delta_3 = 0 \quad \text{2SCus} \quad (6)$$

$$\Delta_3 > \Delta_2 > \Delta_1 > 0 \quad \text{gapless CFL} \quad (7)$$

The 2SCus phase, which was introduced in Ref. [8], must be analyzed for completeness because it and the 2SC phase have the same free energy when $M_s = 0$, and to leading order in M_s if their respective nonzero gap parameters have the same value [8]. However, we shall show in Section III E that the 2SCus phase is never favored, and never gapless.

In the remainder of this paper we construct the free energies and solve the gap equations for the CFL, gapless CFL, 2SC, gapless 2SC [21, 22], and 2SCus phases in an NJL model. We show in detail how the CFL \rightarrow gCFL transition occurs and detail the properties of the gCFL phase. The gCFL phase is a \tilde{Q} -conductor with a nonzero electron density, and these electrons and the gapless quark quasiparticles make the low energy effective theory of the gapless CFL phase and, consequently, its astrophysical properties qualitatively different from that of the CFL phase, even though its $U(1)$ symmetries are the same. Both gapless quasiparticles have quadratic dispersion relations at the quantum critical point. For

values of M_s^2/μ above the quantum critical point, one branch has conventional linear dispersion relations while the other branch remains quadratic, up to tiny corrections. In order to evaluate the range of M_s^2/μ above the critical point within which the gCFL phase remains favored, we construct the 2SC and 2SCus phases and reproduce the 2SC \rightarrow g2SC transition of Refs. [21, 22], here in neutral 3-flavor quark matter, and show that in this context gCFL has a lower free energy than (g)2SC(us). We do not complete the study of mixed phase alternatives, but we do eliminate all the most straightforward possibilities everywhere in the gCFL regime in M_s^2/μ except very close to its upper end, where gCFL, g2SC and unpaired quark matter have comparable free energies. At such large values of M_s^2/μ , however, our pairing ansatz is not sufficiently general to describe all the possibilities, as we discuss in the concluding section of this paper. Before turning to the model analysis, which we detail in Section II and whose results we present in Section III, we conclude this introduction with a model-independent discussion of color and electric neutrality in QCD and with the model-independent argument of Ref. [6].

C. Color and Electric Neutrality in QCD

Stable bulk matter must be neutral under all gauged charges, whether they are spontaneously broken or not. Otherwise, the net charge density would create large electric fields, making the energy non-extensive. In the case of the electromagnetic gauge symmetry, this simply requires zero charge density. In the case of the color gauge symmetry, the formal requirement is that a chunk of quark matter should be a color singlet, i.e., its wavefunction should be invariant under a general color gauge transformation. Color neutrality, meaning equality in the numbers of red, green, and blue quarks, is a less stringent constraint. A color singlet state is also color neutral, whereas the opposite is not necessarily true. However it has been shown that the projection of a color neutral state onto a color singlet state costs no extra free energy in the thermodynamic limit [23]. Analyzing the consequences of the requirement of color neutrality therefore suffices for our purposes.

In nature, electric and color neutrality are enforced by the dynamics of the electromagnetic and QCD gauge fields, whose zeroth components serve as chemical potentials which take on values that enforce neutrality [8, 24]. Since we are limiting ourselves to color neutrality and not color singletness we have to consider only the $U(1) \times U(1)$ diagonal subgroup of the color gauge group. This subgroup is generated by the diagonal generators $T_3 = \text{diag}(\frac{1}{2}, -\frac{1}{2}, 0)$ and $T_8 = \text{diag}(\frac{1}{3}, \frac{1}{3}, -\frac{2}{3})$ of the $SU(3)$ gauge group. Electromagnetism is generated by $Q = \text{diag}(\frac{2}{3}, -\frac{1}{3}, -\frac{1}{3})$ in flavor space (u, d, s). The zeroth components of the respective gauge fields serve as chemical potentials μ_3 and μ_8 coupled to T_3 and T_8 charges, and as an electrostatic potential μ_e coupled to the *negative* elec-

tric charge Q . (We make this last choice so that $\mu_e > 0$ corresponds to a density of electrons, not positrons.) The dynamics of the gauge potentials then require that the charge densities, which are the derivatives of the free energy with respect to the chemical potentials, must vanish:

$$\begin{aligned} Q &= \frac{\partial\Omega}{\partial\mu_e} = 0 \\ T_3 &= -\frac{\partial\Omega}{\partial\mu_3} = 0 \\ T_8 &= -\frac{\partial\Omega}{\partial\mu_8} = 0. \end{aligned} \quad (8)$$

A generic diquark condensate will be neither electrically nor color neutral, so it will spontaneously break these gauge symmetries. However it may be neutral under a linear combination of electromagnetism and color. Indeed, any condensate of the form (2) is neutral with respect to the “rotated electromagnetism” generated by $\tilde{Q} = Q - T_3 - \frac{1}{2}T_8$, so $U(1)_{\tilde{Q}}$ is never broken. This means that the corresponding gauge boson (the “ \tilde{Q} -photon”), a mixture of the ordinary photon and one of the gluons, remains massless. In both the CFL and gCFL phases, the rest of the $SU(3)_{\text{color}} \times U(1)_Q$ gauge group is spontaneously broken, meaning that the combination of the photon and gluons orthogonal to the \tilde{Q} -photon, and all the other gluons, become massive by the Higgs mechanism.

In an NJL model with fermions but no gauge fields, as we shall employ after pursuing model-independent arguments as far as we can, one has to introduce the chemical potentials μ_e , μ_3 and μ_8 “by hand” in order to enforce color and electric neutrality in the same way that gauge field dynamics does in QCD [8].

D. Where does CFL pairing become unstable?

We conclude this introduction with the model-independent argument of Ref. [6] that determines the density at which the CFL phase becomes unstable. The gap equations for the three Δ ’s will turn out to be coupled, but we can, for example, analyze the effect of a specified Δ_1 on the gs and bd quarks without reference to the other quarks. It turns out that gs - bd pairing is the first to break down, and this instability is what catalyzes the CFL \rightarrow gCFL transition.

The leading effect of M_s is like a shift in the chemical potential of the strange quarks, so the bd and gs quarks feel “effective chemical potentials” $\mu_{bd}^{\text{eff}} = \mu - \frac{2}{3}\mu_8$ and $\mu_{gs}^{\text{eff}} = \mu + \frac{1}{3}\mu_8 - \frac{M_s^2}{2\mu}$. In the CFL phase, color neutrality requires $\mu_8 = -M_s^2/2\mu$, a result that is model-independent to leading order in M_s^2/μ^2 [8, 19]. This result can be understood as arising because CFL pairing itself enforces equality in the number of rd and gu quarks, in the number of bu and rs quarks, and in the number of gs and bd quarks [25], but in order to achieve

neutrality the number density of (rd, gu) quarks must be reduced relative to that of the (bu, rs) and (gs, bd) quarks, and this requires a negative μ_8 . Because of the negative μ_8 , $\mu_{bd}^{\text{eff}} - \mu_{gs}^{\text{eff}} = M_s^2/\mu$ in the CFL phase. The CFL phase will be stable as long as the pairing makes it energetically favorable to maintain equality of the bd and gs Fermi momenta, despite their differing effective chemical potentials [25]. It becomes unstable when the energy gained from turning a gs quark near the common Fermi momentum into a bd quark (namely M_s^2/μ) exceeds the cost in lost pairing energy $2\Delta_1$. Hence, the CFL phase is stable when [6]

$$\frac{M_s^2}{\mu} < 2\Delta_{\text{CFL}}. \quad (9)$$

For lower density, i.e. larger M_s^2/μ , the CFL phase must be replaced by some new phase with unpaired bd quarks. One might naively expect this phase to be either neutral unpaired quark matter or neutral 2SC quark matter, but it is known that these have higher free energy than CFL for $M_s^2/\mu < 4\Delta_{\text{CFL}}$ [8, 19], so this new phase, which must have the same free energy as CFL at the critical $M_s^2/\mu = 2\Delta_{\text{CFL}}$, must be something else. In view of its properties that are discussed in detail in Section III, we call it gapless CFL (gCFL).

II. MODEL AND APPROXIMATIONS

We are interested in physics at non-asymptotic densities, and therefore cannot use weak-coupling methods. We are interested in physics at zero temperature and high density, at which the fermion sign problem is acute and the current methods of lattice QCD can therefore not be employed. For this reason, we need to introduce a model in which the interaction between quarks is simplified, while still respecting the symmetries of QCD, and in which the effects of M_s , μ_e , μ_3 and μ_8 on CFL pairing can all be investigated. The natural choice is to model the interactions between quarks using a point-like four-fermion interaction, which we shall take to have the quantum numbers of single-gluon exchange. We work in Euclidean space. Our partition function \mathcal{Z} and free energy density Ω are then defined by

$$\begin{aligned} \mathcal{Z} &= e^{-\beta V \Omega} = \mathcal{N} \int \mathcal{D}\bar{\psi} \mathcal{D}\psi \exp\left(\int \mathcal{L}(x) d^4x\right) \\ \mathcal{L}(x) &= \bar{\psi}(i\cancel{\partial} + \cancel{\mu} - \mathbf{M})\psi - \frac{3}{8}G(\bar{\psi}\Gamma_\mu^A\psi)(\bar{\psi}\Gamma_\mu^A\psi) \end{aligned} \quad (10)$$

where the fields live in a box of volume V and Euclidean time length $\beta = 1/T$, and $\cancel{\mu} = \boldsymbol{\mu}\gamma_4$. The interaction vertex has the color, flavor, and spin structure of the QCD gluon-quark coupling, $\Gamma_\mu^A = \gamma_\mu T^A$. The mass matrix $\mathbf{M} = \text{diag}(0, 0, M_s)$ in flavor space. The chemical potential $\boldsymbol{\mu}$ is a diagonal color-flavor matrix depending on μ , μ_e , μ_3 and μ_8 . The normalization of the four-fermion

coupling $3G/8$ is as in the first paper in Ref. [1]. In real QCD the ultraviolet modes decouple because of asymptotic freedom, but in the NJL model we have to add this feature by hand, through a UV momentum cutoff Λ in the momentum integrals. The model therefore has two parameters, the four-fermion coupling G and the three-momentum cutoff Λ , but it is more useful to parameterize the interaction in terms of a physical quantity, namely the CFL gap parameter at $M_s = 0$ at a reference chemical potential that we shall take to be 500 MeV. We shall call this reference gap Δ_0 . We have checked that if we vary the cutoff Λ by 20% while simultaneously varying the bare coupling G so as to keep Δ_0 fixed, then our results change by a few percent at most. All the results that we present are for $\Lambda = 800$ MeV and for a coupling strength chosen such that $\Delta_0 = 25$ MeV.

We now sketch the derivation of the free energy Ω obtained from the Lagrangian (10) upon making the ansatz (2) for the diquark condensate and working in the mean field approximation. More sophisticated derivations exist in the literature [1], but since we are assuming that the only condensate is of the form (2) we simply Fierz transform the interaction to yield products of terms that appear in (2), and discard all the other terms that arise in the Fierz transformed interaction which would anyway vanish after making the mean field approximation. This yields

$$\mathcal{L}_{\text{int}} = \frac{G}{4} \sum_{\eta} (\bar{\psi} P_{\eta} \bar{\psi}^T) (\psi^T \bar{P}_{\eta} \psi), \quad (11)$$

where

$$(P_{\eta})_{ij}^{\alpha\beta} = C \gamma_5 \epsilon^{\alpha\beta\eta} \epsilon_{ij\eta} \quad (\text{no sum over } \eta) \quad (12)$$

and $\bar{P}_{\eta} = \gamma_4 P_{\eta}^{\dagger} \gamma_4$. The index η labels the pairing channel: $\eta = 1, 2$, and 3 correspond to d - s pairing, u - s pairing, and u - d pairing. The overall coefficient in (11) is the product of the $3G/8$ in (10) and factors of -1 , $4/3$, and $-1/2$ from Fierz transformations in Dirac, color and flavor space, respectively.

Next, for each channel we introduce a complex scalar field ϕ_{η} whose expectation value will be Δ_{η} , the strength of the pairing in the η channel, and bosonize the four-fermion interaction via a Hubbard-Stratonovich transformation. The interaction Lagrangian then becomes

$$\mathcal{L}_{\text{int}} = \frac{1}{2} (\bar{\psi} P_{\eta} \bar{\psi}^T) \phi_{\eta} + \frac{1}{2} \phi_{\eta}^* (\psi^T \bar{P}_{\eta} \psi) - \frac{\phi_{\eta}^* \phi_{\eta}}{G}, \quad (13)$$

where here and henceforth repeated η 's are summed and where it is understood that we are now integrating over the ϕ_{η} as well as ψ and $\bar{\psi}$ in the functional integral (10). The functional integral is now quadratic in the quark fields, so the fermionic function integral can be performed. Since there are terms in the action that can violate quark number, we must use Nambu-Gorkov spinors

$$\Psi = \begin{pmatrix} \psi(p) \\ \bar{\psi}^T(-p) \end{pmatrix}, \quad \bar{\Psi} = \begin{pmatrix} \bar{\psi}(p) & \psi^T(-p) \end{pmatrix} \quad (14)$$

and the full Lagrange density becomes

$$\mathcal{L} = \frac{1}{2} \bar{\Psi} \frac{S^{-1}}{T} \Psi - \frac{\phi_{\eta}^* \phi_{\eta}}{G} \quad (15)$$

where the inverse full propagator is

$$S^{-1}(p) = \begin{pmatrix} \not{p} + \not{\mu} - \mathbf{M} & P_{\eta} \phi_{\eta} \\ \bar{P}_{\eta} \phi_{\eta}^* & (\not{p} - \not{\mu} + \mathbf{M})^T \end{pmatrix}. \quad (16)$$

We now integrate over the fermionic fields to obtain the effective potential for the scalar fields. We also make the mean-field approximation, neglecting fluctuations in the scalar fields and setting ϕ_{η} to its expectation value Δ_{η} . The result is

$$\mathcal{Z} = \left[\text{Det} \frac{S^{-1}(i\omega_n, p)}{T} \right]^{1/2} \exp \left(-\frac{V}{T} \frac{\Delta_{\eta} \Delta_{\eta}}{G} \right) \quad (17)$$

and hence

$$\Omega = -T \sum_n \int \frac{d^3 p}{(2\pi)^3} \frac{1}{2} \text{Tr} \log \left(\frac{1}{T} S^{-1}(i\omega_n, p) \right) + \frac{\Delta_{\eta} \Delta_{\eta}}{G}, \quad (18)$$

where $\omega_n = (2n - 1)\pi T$ are the Matsubara frequencies. We do the Matsubara summation using the identity

$$T \sum_n \ln \left(\frac{\omega_n^2 + \varepsilon^2}{T^2} \right) = |\varepsilon| + 2T \ln(1 + e^{-|\varepsilon|/T}). \quad (19)$$

In the limit of zero temperature only the first term from the right hand side survives, leading to the result

$$\Omega = -\frac{1}{4\pi^2} \int_0^{\Lambda} p^2 \sum_j |\varepsilon_j(p)| dp + \frac{1}{G} (\Delta_1^2 + \Delta_2^2 + \Delta_3^2) - \frac{\mu_e^4}{12\pi^2}, \quad (20)$$

where the electron contribution is included, and $\varepsilon_j(p)$ are the dispersion relations of the quasi-quarks, i.e. the values of the energy at which the propagator diverges:

$$\det S^{-1}(i\varepsilon_j(p), p) = 0. \quad (21)$$

S^{-1} is a 72×72 matrix, but because what occurs in the identity (19) is the combination $\omega^2 + \varepsilon^2$, the sum in (20) is understood to run over 36 roots. (This can be seen as removing the doubling of degrees of freedom introduced by using the Nambu-Gorkov formalism.) In the specific cases where our general ansatz becomes 2SC or CFL pairing, our expression (20) for the free energy, and in particular the coefficient of the Δ^2 term, agrees with the expressions obtained by other methods [1] that do not involve Fierz transformations.

In our numerical evaluation, we omit the antiparticle modes: exciting them costs of order 2μ and they therefore do not play an important role in the physics. This is discussed in more detail below. Neglecting the antiparticles leaves us with only 18 roots of (21) to sum over in (20). These correspond to 9 different dispersion relations

describing the quasiparticles of differing color and flavor, each doubly degenerate due to spin.

A stable, neutral phase must minimize the free energy (20) with respect to variation of the three gap parameters $\Delta_1, \Delta_2, \Delta_3$, meaning it must satisfy

$$\frac{\partial \Omega}{\partial \Delta_1} = 0, \quad \frac{\partial \Omega}{\partial \Delta_2} = 0, \quad \frac{\partial \Omega}{\partial \Delta_3} = 0, \quad (22)$$

and it must satisfy the three neutrality conditions (8). The gap equations (22) and neutrality equations (8) form a system of six coupled integral equations with unknowns the three gap parameters and μ_3, μ_8 and μ_e .

We must now find the dispersion relations $\varepsilon_j(p)$, determined by the zeroes of $\det S^{-1}$ which is specified by (21), (16) with ϕ_η replaced by Δ_η , and (12), then evaluate the free energy Ω using (20), and then solve the six simultaneous equations (8) and (22). Before carrying this calculation through, however, we first make a number of simplifying approximations within the expression for $\det S^{-1}$.

1. We neglect contributions to the condensate that are symmetric in color and flavor: these are known to be present and small [4, 9, 16].
2. We treat the up and down quarks as massless, which is a legitimate approximation in the high density regime, and we treat the constituent strange quark mass M_s as a parameter, rather than solving for an $\langle \bar{s}s \rangle$ condensate. The latter approximation should be improved upon, along the lines of Ref. [19].
3. We incorporate M_s only via its leading effect, namely as a shift $-M_s^2/2\mu$ in the chemical potential for the strange quarks. This approximation neglects the difference between the strange and light quark Fermi velocities, whose effects are known in other contexts to be small [26]. The approximation is controlled by the smallness of M_s^2/μ^2 . For this reason, in all the results that we plot we shall work at $\mu = 500$ MeV and choose a coupling such that the CFL gap at $M_s = 0$ is $\Delta_0 = 25$ MeV. We expect the CFL pairing to break down near $M_s^2 \approx 2\mu\Delta_0$, and choosing $\Delta_0 = \mu/20$ ensures that this occurs where $M_s^2/\mu^2 \sim 1/10$, meaning that we can trust our results well into the gapless CFL phase [27]. If, instead, we choose a larger Δ_0 , as in Ref. [9], we find that our results become markedly more Λ -dependent, which is a good diagnostic for model-dependence.
4. We work to leading nontrivial order in $\Delta_1, \Delta_2, \Delta_3, \mu_e, \mu_3$ and μ_8 . This should be a good approximation, as all these quantities are small compared to μ .
5. We neglect the anti-particles. This simplifies the numerics by discarding physically unimportant degrees of freedom, but one must be cautious with this truncation. It introduces cutoff-dependent terms in our free energy, including some that de-

pend on the chemical potential and therefore introduce cutoff-dependence in the corresponding charges. For our purposes this is not important, firstly because we always present free energy differences relative to neutral unpaired quark matter, and secondly because we only care about electric and color charges that have zero trace over all fermion species, and for these the cutoff dependence cancels out. However, a non-traceless charge like baryon number would have an incorrect cutoff-dependent value when calculated in this approximation.

6. We ignore meson condensation in both the CFL and gCFL phases.

We expect that these approximations have quantitative effects, but none preclude a qualitative understanding of the new phase we shall describe.

We now give the explicit expression for $\det S^{-1}$, after having implemented the approximations above. As described in section IB we use a color-flavor basis in which the gap matrix (3) is conveniently block-diagonal. Since the chemical potential and mass are diagonal in color and flavor, the full inverse propagator (16) is then also block-diagonal in color-flavor space. This means we can break the determinant in equation (21) into four more manageable pieces:

$$\det S^{-1}(p_0, p) = \left(\begin{array}{cccc} D_{ru} & D_{rd} & D_{rs} & D_{gs} \\ & \begin{array}{cc} gd & \\ bs & \end{array} & & \\ & & \begin{array}{cc} gu & \\ bu & \end{array} & \\ & & & \begin{array}{cc} D_{gs} & \\ & bd \end{array} \end{array} \right)^2. \quad (23)$$

We find that the 2×2 determinants are

$$\begin{aligned} D_{rd}^{gu} &= 16\mu^4((\mu_{rd} - p - ip_0)(\mu_{gu} - p + ip_0) + \Delta_3^2) \\ &\quad ((\mu_{rd} - p + ip_0)(\mu_{gu} - p - ip_0) + \Delta_3^2), \\ D_{rs}^{bu} &= 16\mu^4((\mu_{rs} - p - ip_0)(\mu_{bu} - p + ip_0) + \Delta_2^2) \\ &\quad ((\mu_{rs} - p + ip_0)(\mu_{bu} - p - ip_0) + \Delta_2^2), \\ D_{gs}^{bd} &= 16\mu^4((\mu_{bd} - p - ip_0)(\mu_{gs} - p + ip_0) + \Delta_1^2) \\ &\quad ((\mu_{bd} - p + ip_0)(\mu_{gs} - p - ip_0) + \Delta_1^2), \end{aligned} \quad (24)$$

and the 3×3 determinant is

$$\begin{aligned} D_{ru}^{gd} &= a(2\mu)^6 \left(b(de - \Delta_1^2)(cf - \Delta_1^2) - cdf\Delta_2^2 \right. \\ &\quad \left. + d\Delta_1^2\Delta_2^2 - def\Delta_3^2 + f\Delta_1^2\Delta_3^2 \right) \\ &+ (2\mu)^6 \left(\Delta_3^2(de\Delta_2^2 - 4\Delta_1^2\Delta_2^2 + ef\Delta_3^2) \right. \\ &\quad \left. + c(d\Delta_2^4 + f\Delta_2^2\Delta_3^2) \right. \\ &\quad \left. + b(e\Delta_1^2\Delta_3^2 + c(\Delta_1^2\Delta_2^2 - de\Delta_2^2 - ef\Delta_3^2)) \right) \end{aligned} \quad (25)$$

where for compactness we assign

$$\begin{aligned}
a &= \mu_{ru} - p + ip_0 \\
b &= -\mu_{ru} + p + ip_0 \\
c &= \mu_{gd} - p + ip_0 \\
d &= -\mu_{gd} + p + ip_0 \\
e &= \mu_{bs} - p + ip_0 \\
f &= -\mu_{bs} + p + ip_0
\end{aligned} \tag{26}$$

and where we have dropped the superscript on the ‘‘effective quark chemical potentials’’, given by

$$\begin{aligned}
\mu_{ru}^{\text{eff}} &= \mu - \frac{2}{3}\mu_e + \frac{1}{2}\mu_3 + \frac{1}{3}\mu_8, \\
\mu_{gd}^{\text{eff}} &= \mu + \frac{1}{3}\mu_e - \frac{1}{2}\mu_3 + \frac{1}{3}\mu_8, \\
\mu_{bs}^{\text{eff}} &= \mu + \frac{1}{3}\mu_e - \frac{2}{3}\mu_8 - M_s^2/(2\mu), \\
\mu_{rd}^{\text{eff}} &= \mu + \frac{1}{3}\mu_e + \frac{1}{2}\mu_3 + \frac{1}{3}\mu_8, \\
\mu_{gu}^{\text{eff}} &= \mu - \frac{2}{3}\mu_e - \frac{1}{2}\mu_3 + \frac{1}{3}\mu_8, \\
\mu_{rs}^{\text{eff}} &= \mu + \frac{1}{3}\mu_e + \frac{1}{2}\mu_3 + \frac{1}{3}\mu_8 - M_s^2/(2\mu), \\
\mu_{bu}^{\text{eff}} &= \mu - \frac{2}{3}\mu_e - \frac{2}{3}\mu_8, \\
\mu_{gs}^{\text{eff}} &= \mu + \frac{1}{3}\mu_e - \frac{1}{2}\mu_3 + \frac{1}{3}\mu_8 - M_s^2/(2\mu), \\
\mu_{bd}^{\text{eff}} &= \mu + \frac{1}{3}\mu_e - \frac{2}{3}\mu_8.
\end{aligned} \tag{27}$$

These expressions explicitly show how we treat the strange quark mass as a shift in the chemical potential of the strange quarks. In evaluating these determinants, we have extensively used the identity

$$\det \begin{pmatrix} A & B \\ C & D \end{pmatrix} = \det(A) \det(D - CA^{-1}B)$$

for the determinant of a block matrix.

The numerical task is now explicit. We find the quasi-particle dispersion relations $\varepsilon(p)$ by finding the zeros of (23), viewed as a polynomial in p_0 . We then perform the integral in (20) numerically, and obtain Ω . We evaluate the partial derivatives of the free energy required in the neutrality conditions (8) and the gap equations (22) numerically as finite differences, with differences 0.1 MeV in the relevant chemical potential or gap parameter.

As a check, we have also done the calculation of Ω and its partial derivatives by evaluating both the p and p_0 integrals numerically, never writing the latter as a Matsubara sum. In this alternative calculation, we were able to evaluate the partial derivatives in (8) and (22) analytically.

The Ω that we obtain is cutoff dependent, but its partial derivatives (8) and (22) are insensitive to variations in Λ in the sense described above, namely as long as the coupling is changed to keep Δ_0 fixed upon variation in Λ , and as long as Λ is kept well above μ . Furthermore, we are only ever interested in free energy differences between phases. When we evaluate the differences between

the Ω for unpaired, (g)CFL, and (g)2SC quark matter, we find that all such free energy differences are insensitive to the cutoff, as they should be since these differences all reflect physics near the Fermi surfaces. Because we are only interested in free energy differences, in evaluating Ω we make the numerical integral better behaved by subtracting the appropriate expression for neutral unpaired quark matter within the integrand.

The solutions of the system of gap and neutrality equations depend on three parameters: μ , M_s and Δ_0 . Our purpose is to understand the effect of M_s on CFL pairing, and these effects are controlled by the relative size of M_s^2/μ and the gap parameters Δ_i , whose overall magnitude is set by Δ_0 . It is therefore better to think of the three parameters in the problem as μ , M_s^2/μ and Δ_0 . In compact stars, μ increases and M_s presumably decreases, meaning that M_s^2/μ decreases as one approaches the center of the star. For simplicity, we set the overall energy scale in our calculation by fixing $\mu = 500$ MeV, which is reasonable for the center of a neutron star, and vary M_s in order to vary M_s^2/μ . We have confirmed that as long as we choose a Δ_0 that is small enough that the transition (9) occurs where M_s^2/μ^2 corrections are under control, this transition occurs very close to $M_s^2/\mu \approx 2\Delta$, where Δ is gap parameter on the CFL side of the transition. The authors of Ref. [9] have confirmed that this result continues to be valid even for Δ_0 as large as 100 MeV, where the approximations are not as well controlled. We quote results only for $\Delta_0 = 25$ MeV, which is within the plausible range of values that Δ_0 may take in nature [1] and for which our calculation is clearly under control. Although we have obtained our results by varying M_s at fixed μ , we typically quote results in terms of the important combination M_s^2/μ .

III. RESULTS

A. Domain where gCFL is favored

In Figs. 1 and 2, we show the gap parameters and chemical potentials as a function of M_s^2/μ , for $\Delta_0 = 25$ MeV. Fig. 3 shows the free energy. We see a continuous phase transition occurring at a critical M_s^c that, in our model calculation with $\mu = 500$ MeV, lies between $M_s = 153$ MeV and $M_s = 154$ MeV, i.e. at $(M_s^2/\mu)_c \approx 47.1$ MeV. This agrees exceedingly well with the expected value 2Δ from Eq. (9), since on the CFL side of the transition $\Delta_1 = \Delta_2 = \Delta_3 = 23.5$ MeV. For $M_s^2/\mu < (M_s^2/\mu)_c$, the CFL phase is favored, with all three gaps equal to each other within our approximations. If we improve upon our approximate treatment of M_s , we expect $\Delta_1 = \Delta_2$ with these gap parameters slightly smaller than Δ_3 , because Δ_1 and Δ_2 describe pairing between quarks with differing Fermi velocities, an effect of M_s that we are neglecting because it is known to be small in other contexts [26]. (Indeed, it proves to be a few percent effect also in the present context [27].)

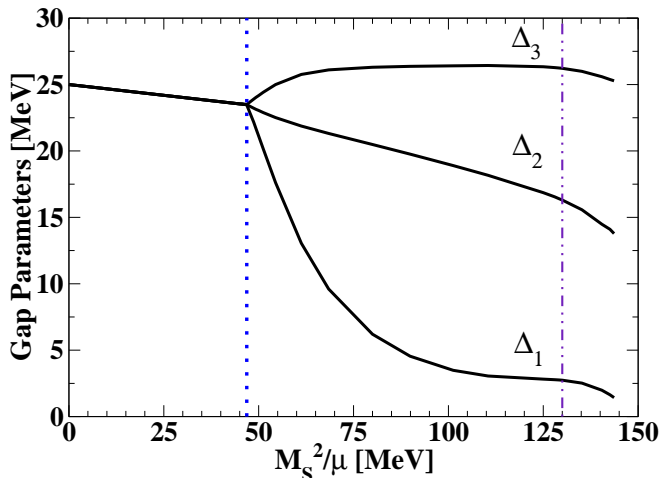


FIG. 1: Gap parameters Δ_3 , Δ_2 , and Δ_1 as a function of M_s^2/μ for $\mu = 500$ MeV, in a model where $\Delta_0 = 25$ MeV (see text). At $M_s^2/\mu \approx 47.1$ MeV (vertical dotted line) there is a continuous phase transition between the CFL phase and a phase that we shall identify below as the gapless CFL phase. We find gapless CFL phase solutions up to $M_s^2/\mu \approx 144$ MeV. But, we shall see in Fig. 3 that above $M_s^2/\mu \approx 130$ MeV (which we denote here with a vertical dash-dotted line) unpaired quark matter has a lower free energy than the gapless CFL phase.

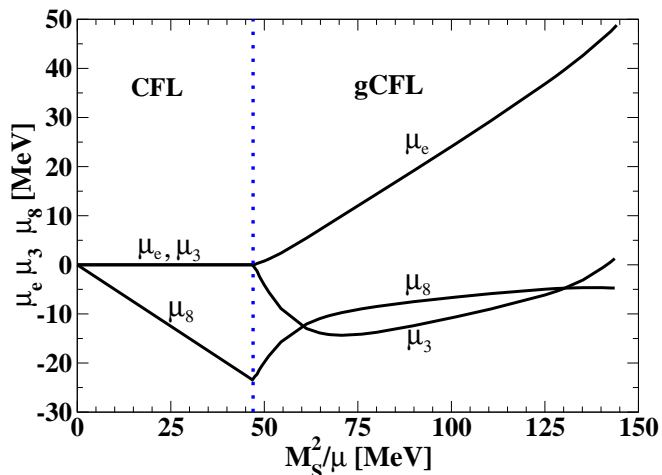


FIG. 2: Chemical potentials μ_e , μ_3 and μ_8 as a function of M_s^2/μ in the CFL/gCFL phase for the same parameters as in Fig. 1. The effects of electrons on the free energy have been included in the calculation, as will be discussed in more detail below. We see that the gapless CFL phase has $\mu_e > 0$, meaning that it has a nonzero density of electrons. Perhaps the most physically relevant order parameter for the CFL/gCFL phase transition is the electron number density $n_e \sim \mu_e^3$.

For $M_s^2/\mu < (M_s^2/\mu)_c$ our results agree with the small- M_s expansion of Ref. [8], where $\mu_3 = \mu_e = 0$ and $\mu_8 =$

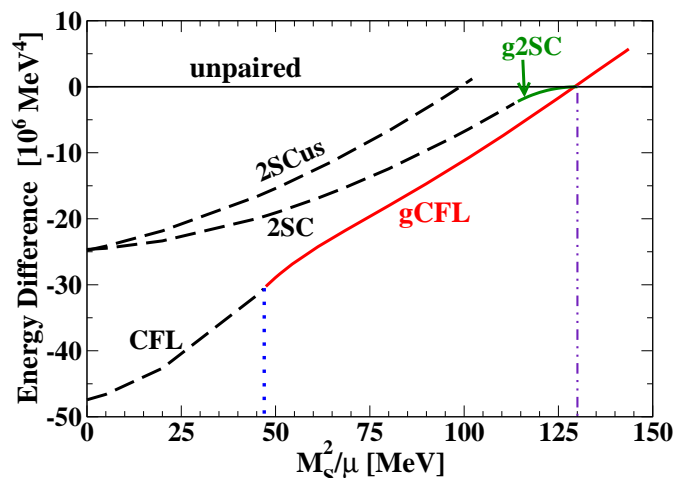


FIG. 3: Free energy of the CFL/gCFL phase, relative to that of neutral noninteracting quark matter and that of the 2SC/g2SC and 2SCus phases, discussed in Section III E. There is a CFL→gCFL transition at $(M_s^2/\mu)_c \approx 47.1$ MeV, (vertical dotted line), at which the free energy and its slope are continuous, indicating that the transition is not first order. If we neglect the possibility of other phases (for example g2SC) we would conclude from this figure that there is a first order transition gCFL→unpaired at $M_s^2/\mu \approx 130$ MeV (vertical dash-dotted line).

$-M_s^2/(2\mu)$ and the free energy is

$$\begin{aligned} \Omega_{\text{CFL}}^{\text{neutral}} &= -\frac{3\mu^4}{4\pi^2} + \frac{3M_s^2\mu^2}{4\pi^2} - \frac{1 - 12 \log(M_s/2\mu)}{32\pi^2} M_s^4 \\ &\quad - \frac{3\Delta^2\mu^2}{\pi^2} \\ &= \Omega_{\text{unpaired}}^{\text{neutral}} + \frac{3M_s^4 - 48\Delta^2\mu^2}{16\pi^2}. \end{aligned} \quad (28)$$

As the density decreases (i.e. as M_s^2/μ increases) through the CFL→gCFL transition, the gap parameters split apart, with Δ_3 increasing slightly and Δ_2 and Δ_1 dropping significantly, with Δ_1 dropping faster than Δ_2 .

We have verified that $M_s^2/\mu\Delta$ is the relevant dimensionless quantity by changing the coupling strength, i.e. picking a different Δ_0 (gap at $M_s = 0$). The critical point $(M_s^2/\mu)_c$ changes as predicted by (9). Furthermore we checked the robustness of our results upon variation of the cutoff Λ , observing changes of only a few percent in the value of $M_s^2/\mu\Delta$ at the transition upon changing Λ by up to 20% while keeping Δ_0 fixed.

Fig. 3 confirms that the slope of the free energy is continuous at the CFL/gCFL transition, indicating that it is not first order. We have not determined the order of the transition, because evaluating higher derivatives of the free energy with respect to M_s^2/μ is not numerically feasible. The most physically relevant order parameter is the electron density $n_e \sim \mu_e^3$, which is of course equal in magnitude to the electric charge density of the quarks. This increases above the transition like

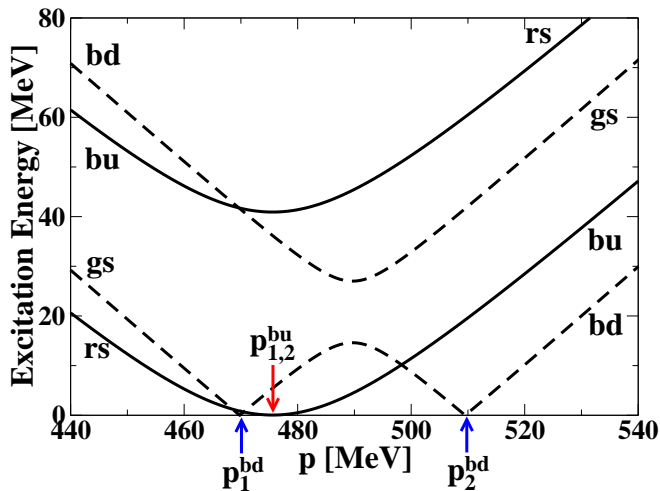


FIG. 4: Dispersion relations at $M_s^2/\mu = 80$ MeV (with μ and Δ_0 as in previous figures) for the quasiparticles that are linear combinations of gs and bd quarks (dashed lines) and for the quasiparticles that are linear combinations of bu and rs quarks (solid lines). There are gapless gs - bd modes at $p_1^{bd} = 469.8$ MeV and $p_2^{bd} = 509.5$ MeV, which are the boundaries of the “blocking” [29, 30] or “breached pairing” [31] region wherein there are unpaired bd quarks and no gs quarks. One bu - rs mode is gapless at $p = 475.6$ MeV with an almost exactly quadratic dispersion relation that we shall discuss below.

$n_e \sim [(M_s^2/\mu) - (M_s^2/\mu)_c]^3$, suggesting a fourth order phase transition! This argument neglects the small electron mass and, furthermore, it neglects the fact that, as we shall see in Eq. (33), there is also a nonzero number density of neutral unpaired quark quasiparticles that grows like $[(M_s^2/\mu) - (M_s^2/\mu)_c]^{1/2}$. Although because these unpaired quasiparticles are neutral they are less important phenomenologically, this does suggest that the transition is second order, as in the analysis of Ref. [28].

If we had used a simpler ansatz in which the gap parameters were constrained to one value $\Delta \equiv \Delta_1 = \Delta_2 = \Delta_3$, then the CFL phase would have remained artificially stable above the critical value of M_s^2/μ . From Eq. (28), its free energy would be higher than that of gCFL, rising to equality with that of unpaired quark matter at a value of M_s^2/μ around 90 MeV. (The precise value depends on how the common Δ changes with M_s .)

Of course, we actually used the more general ansatz (2) that allows the Δ 's to differ. We found that the CFL phase becomes unstable and is replaced by the gCFL phase, in which the gaps have very different values, so the simplified analysis of Ref. [8] does not apply. The free energy of the gCFL phase crosses that of unpaired quark matter at $M_s^2/\mu \approx 130$ MeV. This phase transition is first order, and we are able to follow the metastable gCFL phase up to $M_s^2/\mu = 144$ MeV where, as we shall explain below, it ceases to be a solution.

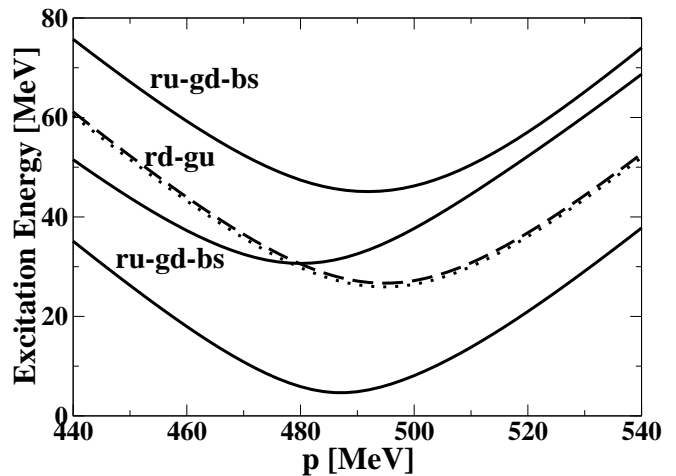


FIG. 5: Dispersion relations at $M_s^2/\mu = 80$ MeV for the two quasiparticles that are linear combinations of rd and gu quarks (dashed and dotted), and for the three quasiparticles that are linear combinations of ru , gd and bs quarks (solid). These five quark quasiparticles all have gaps throughout the CFL and gCFL phases.

B. The nature of the gCFL phase

Up to this point we have not justified our use of the name “gapless CFL” for the new phase that replaces the CFL phase at $M_s^2/\mu \gtrsim 2\Delta$. We have given model-independent arguments to expect that it will contain unpaired bd quarks, but now we describe its properties in more detail. In calculating the free energy (20) of the Cooper-paired quark matter we automatically obtain the quasiquark dispersion relations (21), so we can see what gapless modes exist. These modes are important because, at the temperatures $T \lesssim$ keV characteristic of neutron stars, only the lightest modes will contribute to transport properties.

In Fig. 4 we show the dispersion relations for the rs - bu and gs - bd 2×2 blocks in the quasiquark propagator, at $M_s^2/\mu = 80$ MeV. We see immediately that there are gapless modes in both blocks, justifying our name for this phase. Before moving on to a detailed discussion of the physical properties of the gCFL phase, we should note that the phenomenon of gapless superconductivity is well known, at least theoretically. It was first suggested by Sarma [32] who worked in a context much like our gs - bd block in isolation, and found that the gapless superconducting phase is never stable. Alford, Berges and Rajagopal found a metastable gapless color superconducting phase in Ref. [33], but this phase was neither electrically nor color neutral. The key observation was made by Shovkovy and Huang [21], who discovered that when the constraints of electric and color neutrality are imposed on the 2SC phase in two-flavor QCD, there are regions of parameter space where a gapless color superconducting phase is stable. Following their nomenclature (they described a “gapless 2SC phase”) we refer to the phase that we find above M_s^2/μ as the “gapless color-flavor

locked phase” [6].

Gapless two-flavor color superconductivity was also studied in Ref. [31], building upon prior work done in a cold atom context [34]. These authors analyzed pairing between a heavy and a light quark, akin to gs and bd , in the case in which the gs quarks are nonrelativistic. They find that a gapless phase (they describe the blocking region as a region in which pairing is “breached”) is stable if the relative density of the two species is held fixed.

Note that in our three-flavor calculation, both the gap equations (22) and the neutrality conditions (8) couple all nine quarks. Although the single particle dispersion relations can be analyzed for the gs and bd quarks in isolation, and are qualitatively similar to those obtained in Refs. [21, 31] in a two-flavor setting, the implications of neutrality are more subtle in our three-flavor context as we shall explain below.

Each of the dispersion relations in Figs. 4 and 5 describes an excitation with well-defined \tilde{Q} , although the sign of \tilde{Q} changes at momenta where the dispersion relation is gapless. Beginning with an example with no gap, the upper solid curve in Fig. 4 describes excitations that are linear combinations of rs particles and bu holes, both with $\tilde{Q} = -1$. The lower dashed curve in Fig. 4 has clearly visible momenta p_1^{bd} and p_2^{bd} where it is gapless, so we use this as an example of “sign change” even though it describes $\tilde{Q} = 0$ quasiparticles: to the left of p_1^{bd} , it describes gs -holes with a very small admixture of bd particles; to the right of p_2^{bd} , it describes bd particles with a very small admixture of gs holes; but, between p_1^{bd} and p_2^{bd} it describes excitations that are superpositions of bd holes and gs particles.

In the CFL phase, once we take into account the explicit symmetry breaking introduced by the strange quark mass and electromagnetism, the unbroken symmetry is reduced from the diagonal $SU(3)_{L+R+c}$ to $U(1)_{\tilde{Q}} \times U(1)$ [12]. The last $U(1)$ corresponds to “color + flavor hypercharge” and may be spontaneously broken by meson condensation [13]. The gapless CFL phase has the same symmetry as the CFL phase, and it will therefore be interesting to investigate the possibility of meson condensation in the gCFL phase. The effective theory for the Goldstone bosons alone will have the same form as in the CFL phase, albeit with new contributions to their masses coming from the differences between the values of the three Δ_i^2 . And, furthermore, the gapless quasiparticles must be included in the low energy effective theory.

1. Dispersion relations, gapless modes, and neutrality

As will soon become clear, the 3×3 block in the pairing pattern (3) plays a minor role: its quasiparticles are always gapped, so we mainly discuss the three 2×2 blocks. In general, when two species of massless quarks undergo s -wave pairing with gap parameter Δ , the dispersion re-

quark pair	$\delta\mu_{\text{eff}}$	$\delta\mu_{\text{eff}}$ in electronless CFL
$rd-gu$	$\frac{1}{2}(\mu_e + \mu_3)$	μ_e
$rs-bu$	$\frac{1}{2}(\mu_e + \frac{1}{2}\mu_3 + \mu_8 - \frac{1}{2}M_s^2/\mu)$	$\mu_e - \frac{1}{2}M_s^2/\mu$
$gs-bd$	$\frac{1}{2}(\frac{1}{2}\mu_3 - \mu_8 + \frac{1}{2}M_s^2/\mu)$	$M_s^2/2\mu$

TABLE I: Chemical potential splittings for the 2×2 pairing blocks. ($\delta\mu_{\text{eff}}$ and $\bar{\mu}$, which is not tabulated, are defined in each row such that the effective chemical potentials of the two quarks that pair are $\bar{\mu} \pm \delta\mu_{\text{eff}}$.) The middle column gives $\delta\mu_{\text{eff}}$ for general values of the chemical potentials μ_e , μ_3 and μ_8 . In the last column, it is understood that as μ_e is varied, μ_3 and μ_8 “follow it” in such a way that varying μ_e corresponds to varying $\mu_{\tilde{Q}}$, tracking degenerate \tilde{Q} -neutral solutions for electron-less CFL quark matter.

lations of the two resulting quasiparticles are

$$E(p) = \left| \delta\mu \pm \sqrt{(p - \bar{\mu})^2 + \Delta^2} \right| \quad (29)$$

where the individual chemical potentials of the quarks are $\bar{\mu} \pm \delta\mu$. As long as the chemical potentials pulling the two species apart are not too strong, Cooper pairing occurs at all momenta:

$$\text{pairing criterion: } |\delta\mu| < \Delta. \quad (30)$$

However when this condition is violated there are gapless ($E = 0$) modes at momenta

$$p_{\text{gapless}} = \bar{\mu} \pm \sqrt{\delta\mu^2 - \Delta^2} \quad (31)$$

and there is no pairing in the “blocking” or “breached pairing” region between these momenta [21, 29, 30, 31, 34]. (The identification of the boundaries of a blocking region with locations in momentum space where a dispersion relation is gapless is discussed with considerable care in Ref. [30], which considers a more complicated setting in which rotational symmetry is spontaneously broken and the blocking regions are not spherically symmetric. Such blocking regions were analyzed previously in Refs. [29].) The pairing criterion (30) can be interpreted as saying that the free energy cost 2Δ of breaking a Cooper pair of two quarks a and b is greater than the free energy $2\delta\mu$ gained by emptying the a state and filling the b state (assuming that $\delta\mu$ pushes the energy of the a quark up and the b quark down) [25]. In the blocking region, we find unpaired b quarks and no a quarks.

We wish now to apply these ideas to the 2×2 pairing blocks in three-flavor quark matter, first in the CFL phase. As described above, neutrality is imposed via chemical potentials μ_e, μ_3, μ_8 , and in the CFL phase the leading effect of the strange quark mass is an additional effective chemical potential $-M_s^2/2\mu$ for the strange quarks. The splittings of the various pairs are then as given in the middle column of table I.

Electrons will play a crucial role in understanding the gCFL phase, but it is fruitful initially to consider matter

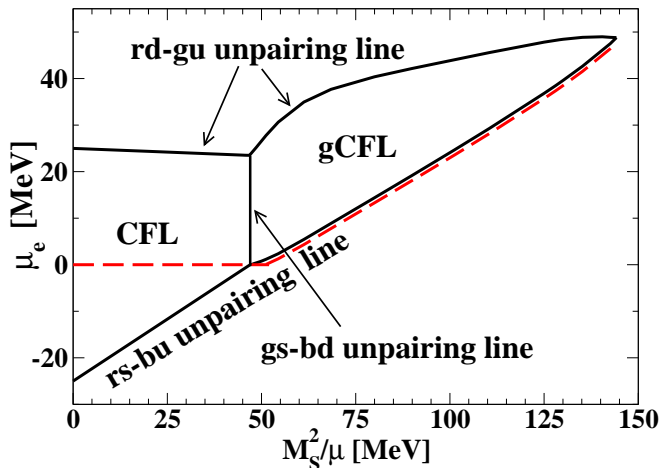


FIG. 6: Unpairing lines for the same parameters as used in Fig. 1. If electrons are neglected, then the upper and lower curves bound the region of μ_e where neutral solutions to the gap equations are found. These solutions are all \tilde{Q} -insulators. Taking electrons into account, the correct solution is the dashed line: in the CFL phase $\mu_e = 0$, while the gCFL phase corresponds to values of μ_e below but very close to the rs - bu unpairing line. gCFL is a \tilde{Q} -conductor both because of the nonzero electron density and because of the ungapped \tilde{Q} -charged rs - bu quasiparticles.

consisting only of quarks, which we can do by sending the electron mass to infinity. In the absence of electrons, at each M_s^2/μ there is a plateau in the free energy of neutral CFL (or gCFL) solutions: if we vary the chemical potential that couples to \tilde{Q} charge,

$$\mu_{\tilde{Q}} = -\frac{4}{9}(\mu_e + \mu_3 + \frac{1}{2}\mu_8), \quad (32)$$

while keeping constant the gap parameters Δ_i and the two orthogonal combinations of chemical potentials, then over a range of $\mu_{\tilde{Q}}$ the free energy does not change and we have a family of neutral stable solutions to the gap equations. This indicates that, in the absence of electrons, both the CFL and gCFL phases are \tilde{Q} -insulators. On this plateau, all \tilde{Q} -charged quasiparticles remain gapped: (30) is obeyed for the (rd, gu) and (rs, bu) 2×2 quark pairing blocks. At the edges of the plateau, some \tilde{Q} -charged quasiparticles become gapless, the material ceases to be \tilde{Q} -neutral, $\partial\Omega/\partial\mu_{\tilde{Q}} \neq 0$, and the free energy is no longer independent of changes in $\mu_{\tilde{Q}}$. The range of $\mu_{\tilde{Q}}$ that defines the plateau is therefore the band gap for the CFL/gCFL insulator. In Fig. 6 we show the unpairing lines for each 2×2 quark pairing block. The rd - gu line and the rs - bu line bound the plateau region. Although the vertical axis is labelled “ μ_e ”, it actually corresponds to variation in $\mu_{\tilde{Q}}$, since we varied (μ_e, μ_3, μ_8) by a multiple of $(1, 1, \frac{1}{2})$. In the CFL phase, this corresponds to keeping $\mu_3 = \mu_e$ and $\mu_8 = \frac{1}{2}(\mu_e - M_s^2/\mu)$ while varying μ_e .

We see that (g)CFL matter exists in a wedge, between the rd - gu unpairing line and the rs - bu unpairing line. From table I we can see that the bd - gs -unpairing line

is vertical because the bd and gs quasiparticles are \tilde{Q} -neutral, so their splitting depends only on M_s^2/μ and not on μ_e . This unpairing line has a different character than the other two. Rather than bounding the band-gap within which solutions are found, it separates the CFL and gCFL phases. CFL is stable only up to a critical value of M_s^2/μ , where the gs - bd pairs break.

At the lower (rs - bu -unpairing) line, $\mu_{\tilde{Q}}$ is large enough that the bu and rs quarks, which have $\tilde{Q} = +1$ and $\tilde{Q} = -1$ respectively and which pair with gap parameter Δ_2 , no longer pair completely: it is energetically favorable to create a new blocking region of unpaired bu quarks. At this \tilde{Q} -electrostatic potential, the CFL \tilde{Q} -insulator breaks down, unpaired bu quarks with $\tilde{Q} = +1$ are created, the free energy is no longer $\mu_{\tilde{Q}}$ -independent, and in fact the neutrality conditions and gap equations are no longer satisfied.

At the upper (rd - gu -unpairing) line, $\mu_{\tilde{Q}}$ is so low that the rd and gu quarks, which have $\tilde{Q} = -1$ and $\tilde{Q} = +1$ respectively and which pair with gap parameter Δ_3 , no longer pair completely, and it is energetically favorable to create a new blocking region of unpaired rd quarks, and once again no solution is found.

At $M_s^2/\mu = 143$ MeV, which is so large that the gapless CFL phase is anyway already metastable with respect to unpaired quark matter, the two boundaries cross, meaning that no gapless CFL solution can be found.

So, in the absence of electrons, we can find stable solutions of the gap and neutrality equations everywhere between the rs - bu and rd - gu curves in Fig. 6. To the left of the gs - bd unpairing line this is the CFL phase, a \tilde{Q} -insulator with no gapless quasiquark modes. To the right of that line we have the gCFL phase, again a \tilde{Q} -insulator, in which all \tilde{Q} -charged modes are gapped, but there are $\tilde{Q} = 0$ gapless quasiparticles.

We now restore the electrons, setting their mass to zero. In the CFL region, the system is forced to $\mu_e = 0$ (dashed line in Fig. 6) [25]. However, at the transition point to gCFL, where the gs - bd pairs break, we find that the neutrality requirement forces us over the line where rs - bu pairs also begin to break. The result is that as M_s^2/μ increases further, the system maintains neutrality by staying close to the rs - bu -unpairing line, where there is a narrow blocking region in which there are unpaired bu quarks. Their charge is cancelled by a small density of electrons. We analyze this quantitatively below.

We see that real-world gCFL quark matter is a conductor of \tilde{Q} charge, since it has gapless \tilde{Q} -charged quark modes, as well as electrons. The rd and gu quarks, which are insensitive to the strange quark mass, remain robustly paired and the \tilde{Q} -neutral bd and gs quarks develop a large blocking region as the system moves far beyond their unpairing line. The neutrality requirement naturally keeps the system close to the rs - bu -unpairing line, following the dashed line in Fig. 6, so these quarks have a very narrow blocking region and an almost quadratic dispersion relation (see below). Although $U(1)_{\tilde{Q}}$ is unbroken in the gapless CFL phase, the presence of electrons and un-

paired bu quarks makes this phase a \tilde{Q} -conductor. This is in contrast to the CFL phase, which is a \tilde{Q} -insulator with no gapless quasiquarks and no electrons.

The gapless quark quasiparticles occur in the gs - bd and rs - bu sectors. Since these will have a dramatic effect on transport properties, we now discuss them in greater depth.

2. The gs - bd sector

In a typical part of the gCFL phase space, the \tilde{Q} -neutral gs - bd sector is well past its unpairing line, and there is a large blocking region between momenta p_1^{bd} and p_2^{bd} at which there are gapless excitations, as shown in Fig. 4. In the blocking region $p_1^{bd} < p < p_2^{bd}$ there are bd quarks but no gs quarks, and thus no pairing. We have confirmed this by direct evaluation of the difference between the number density of bd and gs quarks, showing this to be equal to the volume of the blocking region in momentum space.

Note that even though there is no pairing in the ground state in the blocking region, the dispersion relations are not trivial. Because the states obtained via the two different single particle excitations that are possible (adding a gs quark or removing a bd quark) mix via the Δ_1 condensate, the two dispersion relations exhibit an “avoided crossing” between p_1^{bd} and p_2^{bd} . If we neglect the mixing among the excitations introduced by Δ_1 , the gapless excitations just above (below) p_2^{bd} are bd quarks (holes) and those just above (below) p_1^{bd} are gs quarks (holes).

It may seem coincidental that the value of M_s^2/μ at which the CFL phase becomes gapless is the same as the value at which Δ_1 and Δ_2 separate in Fig. 1. Although we do not see a profound reason for this, it is certainly not a coincidence. The CFL \rightarrow gCFL transition is triggered by the instability of the CFL phase that occurs when a gs - bd quasiparticle dispersion relation goes gapless, indicating the instability towards gs - bd unpairing and the opening up of a blocking region in momentum space, filled with unpaired bd quarks and with no gs - bd pairing. Consequently, one of the terms in the Δ_1 gap equation — that corresponding to the gs - bd block — is reduced in magnitude because its integrand vanishes within the blocking region. This reduction in the support of the Δ_1 gap equation integrand causes Δ_1 to drop.

The “thickness” of the bd blocking region can be considered an order parameter for gCFL: for M_s^2/μ below the critical value there is no blocking region. Just above the critical value we can use the results of table I and (31) to show that

$$p_2^{bd} - p_1^{bd} \sim \Delta_1^{1/2} \left(\frac{M_s^2}{\mu} - \frac{(M_s^c)^2}{\mu} \right)^{1/2} \sim (M_s - M_s^c)^{1/2}, \quad (33)$$

typical behavior for a second order phase transition. Because we are analyzing a zero temperature quantum

phase transition, the long wavelength physics at the critical point is 4-dimensional rather than 3-dimensional as at a finite temperature transition.

3. The rs - bu sector

As discussed above, the gCFL phase remains neutral by crossing the rs - bu unpairing line, and developing enough unpaired bu quarks to cancel the \tilde{Q} charge of the electrons. The electrons contribute $(-\mu_e^4/12\pi^2)$ to the free energy, so \tilde{Q} -neutrality can be maintained as long as

$$n_e = \frac{\mu_e^3}{3\pi^2} = n_{bu} = \frac{(p_2^{bu})^3 - (p_1^{bu})^3}{3\pi^2}, \quad (34)$$

where p_1^{bu} and p_2^{bu} bound the blocking region of unpaired bu quarks. The condition (34) implies that

$$(p_2^{bu} - p_1^{bu}) = \frac{\mu_e^3}{3\bar{p}^2} \quad (35)$$

where \bar{p} is the average of p_1^{bu} and p_2^{bu} . At $M_s^2/\mu = 80$ MeV, where $\mu_e = 14.6$ MeV at the lower curve in Fig. 6, this implies $(p_2^{bu} - p_1^{bu}) = 0.0046$ MeV! Indeed, in Fig. 4 the separation between p_1^{bu} and p_2^{bu} is invisible, and the dispersion relation appears to be quadratic about a single gapless point. To resolve the separation between p_1^{bu} and p_2^{bu} , we did calculations assuming 200 and 500 “flavors” of massless electrons. In these cases, $(p_2^{bu} - p_1^{bu}) \sim 1$ MeV and ~ 3 MeV, in very good agreement with the above argument. Returning to our world with its single electron species, because $(p_2^{bu} - p_1^{bu})$ is so small, the value of μ_e at the true \tilde{Q} -neutral solution is *very* close to that given by the lower curve in Fig. 6. And, the gaps are *very* close to those found in a calculation done in the absence of electrons.

From Eq. (29), the maximum in the quasiparticle energy between the two gapless momenta is $E_{\max} = |\delta\mu - \Delta|$, so from (31) we can express this in terms of the width of the blocking region: $4(|\delta\mu| + \Delta)E_{\max} = (p_2 - p_1)^2$. For the rs - bu quarks, the blocking region is always very narrow, so $E_{\max} \approx (p_2^{bu} - p_1^{bu})^2/(8\Delta_2)$ which from (35) is a small fraction of an electron volt at $M_s^2/\mu = 80$ MeV. Thus, at any astrophysically relevant temperature, the rs - bu dispersion relation can be treated as quadratic about a single momentum at which it is gapless. Indeed, even at $M_s^2/\mu = 130$ MeV where the gapless CFL phase ceases to be the ground state, $\mu_e = 40.3$ MeV, $(p_2^{bu} - p_1^{bu}) \sim 0.1$ MeV and the peak of the dispersion relation between p_1^{bu} and p_2^{bu} is at about 50 eV. The requirement of \tilde{Q} -neutrality naturally forces this dispersion relation to be *very* close to quadratic, without requiring fine tuning to a critical point.

4. The rd - gu sector and the 3×3 ru - gd - bs block

In Fig. 5 we show the dispersion relations for the quasiparticles in the rd - gu sector. One of these becomes gapless at the upper boundary of the wedge in Fig. 6, but we have seen that in the presence of electrons, the neutral gapless CFL solution is never near this upper boundary. Therefore, these dispersion relations are always gapped, as in the figure. In Fig. 5 we also show the dispersion relations for the three quasiparticles from the 3×3 block. These quasiparticles carry zero \tilde{Q} charge and they always have nonzero gap. Their smallest gap becomes very small near the rightmost tip of the gCFL wedge region in Fig. 6, but is always greater than 1 MeV in the region in which gCFL is favored.

C. The gCFL Free Energy Function

In the previous subsection, we have used the dispersion relations to delineate the unpairing lines which bound the ranges in $\mu_{\tilde{Q}}$ where, in the absence of electrons, \tilde{Q} -insulator solutions are to be found and which separate the CFL and gCFL phases. Here, we sketch the behavior of the free energy Ω in the vicinity of solutions to the gap and neutrality equations, and see how this behavior changes at the unpairing lines.

In Fig. 7 we study the free energy in the vicinity of a gapless CFL solution not far above the CFL \rightarrow gCFL transition. We have neglected electrons in making this plot; the change from including them would be invisible on the scale of the plot. We plot the free energy upon variation of gap parameters while keeping μ 's fixed (dashed curves in Fig. 7), and we also plot the “neutral free energy” (solid curves) obtained by varying gap parameters about the solution while solving the neutrality conditions anew for each value of the gap parameters. We see that the solution is a minimum of the neutral free energy, confirming that we have succeeded in finding a stable neutral solution. However, the solution is not at a minimum of the free energy upon variation of the gap parameters while keeping μ 's fixed.

We see in the top panel of Fig. 7 that the solution is found at a local maximum of the dashed curve describing variation of Δ_1 at fixed μ 's. Shovkovy and Huang described similar behavior in the gapless 2SC case in Refs. [21, 22], and suggested that this is a characteristic of gapless superconductivity. We find this *not* to be the case: deep in the gCFL phase, at $M_s^2/\mu = 80$ MeV rather than the $M_s^2/\mu = 51.2$ MeV of Fig. 7, we find that the gCFL solution is a local minimum of both the dashed and the solid curves in the analogue of the top panel of Fig. 7. That is, we find an onset of the behavior seen in the top panel of Fig. 7 as we cross the CFL \rightarrow gCFL transition, namely the gs - bd unpairing line: as a gs - bd blocking region begins to open up, the solution goes from being a local minimum of the dashed curve to being a local maximum. However, we find that the dashed curve

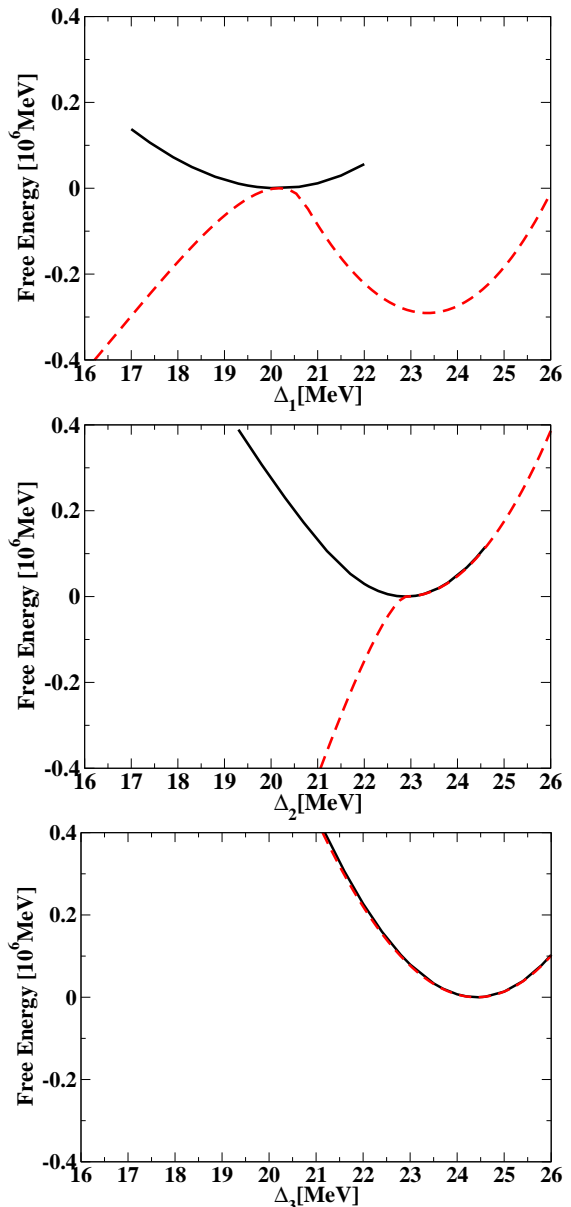


FIG. 7: These figures show the free energy Ω in the vicinity of the gapless CFL solution for $M_s^2/\mu = 51.2$ MeV. In each panel, the dashed curve is obtained by varying one of the gap parameters (Δ_1 in the top panel, Δ_2 in the middle; Δ_3 in the bottom) while keeping the other two gap parameters and the chemical potentials μ_e , μ_3 and μ_8 fixed. The free energies are measured relative to that of the solution. The solid curve in each panel depicts the “neutral free energy”, obtained by varying one gap parameter, keeping the other gap parameters fixed, and solving the neutrality conditions anew for each point on the solid curve.

does not persist in this shape as the gs - bd blocking region expands. The *onset* of gaplessness is characterized by a dashed curve as in the top panel of Fig. 7, but gaplessness itself need not be.

In the middle panel of Fig. 7, we find that the solution is at a point of inflection with respect to variation of

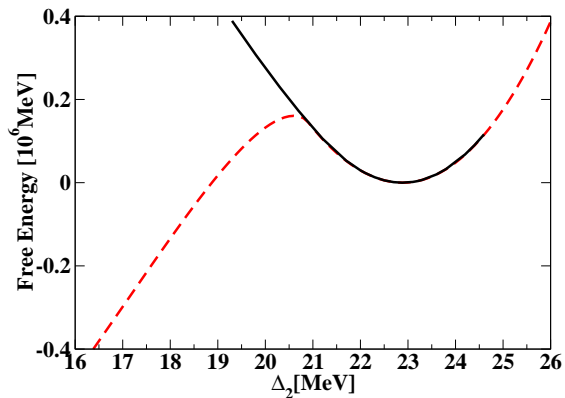


FIG. 8: Same as the middle panel of Fig. 7, except that μ_e has been increased by 2 MeV while changing μ_3 and μ_8 so as to make this a shift in $\mu_{\bar{Q}}$. This means that, neglecting electrons, we are now exploring the change of the free energy and the neutral free energy upon variation of Δ_2 about a gCFL solution that is in the interior of the wedge in Fig 6, rather than at its bottom boundary.

Δ_2 at fixed μ 's. We find that the gCFL solutions at all values of M_s^2/μ above $(M_s^2/\mu)_c$ are at points of inflection of this sort. This arises because a gCFL solution is forced by the neutrality constraint to be very close to the *bu-rs* unpairing line. In Fig. 8 we replot the middle panel of Fig. 7 after increasing μ_e by 2 MeV while varying μ_3 and μ_8 so that only $\mu_{\bar{Q}}$ changes. This means that we have taken a 2 MeV step upwards in Fig. 6, away from the *bu-rs* unpairing line. And, we see that the solution is now a minimum with respect to variation of Δ_2 at fixed μ 's. The point of inflection has resolved itself into a minimum and a maximum, with the solution at the minimum. Thus, the point of inflection in the dashed curve does indeed occur at the *bu-rs* unpairing line.

Note that at $M_s^2/\mu = 80$ MeV, once we have taken an upward step away from the *bu-rs* unpairing line in Fig. 6, obtaining the analogue of Fig. 8, the gapless CFL phase solution is now a local minimum of both the dashed and solid curves for variation in the Δ_1 , Δ_2 and Δ_3 directions.

If we take a step in the “wrong direction” in Fig. 6, downwards from the *bu-rs* unpairing line, the point of inflection in the middle panel of Fig. 7 vanishes and the dashed curve becomes monotonically increasing, indicating that there is no solution to the Δ_2 gap equation to be found at these values of the μ 's. In the presence of electrons, the neutrality conditions are satisfied *just* below the *bu-rs* unpairing line in Fig. 6, and the dependence of the free energy on Δ_2 is slightly modified so that the point of inflection in the middle panel of Fig. 7 occurs where the neutrality conditions are satisfied. We have confirmed this in calculations done with 200 and 500 species of electrons; with a single species as in the real world, the changes in Fig. 7 are invisible on the scales of the plot.

Finally, with respect to variation of Δ_3 , the solution is a local minimum of the dashed curve in the lower panel of Fig. 7. However, we have verified that if we move

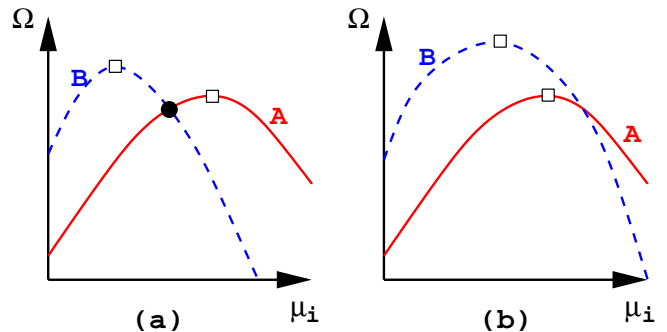


FIG. 9: Schematic illustration of conditions for the occurrence of mixed phases. Free energy Ω for two phases A and B is shown as a function of some chemical potential μ_i . Charge $Q_i = -\partial\Omega/\partial\mu_i$ is given by the slope. Squares mark the neutral points. Panel (a): at the neutral point for each phase, the other phase has lower free energy, so there is a point (black dot) where the two phases can coexist with the same pressure and opposite charge, with lower free energy than either neutral phase. Depending on Coulomb and surface energy costs, a mixed phase may exist there. Panel (b): phase B has higher free energy than phase A at the point where A is neutral. At no point do the two phases coexist with opposite charge, so no mixed phase is possible.

sufficiently upwards in Fig. 6 as to run into the *rd-gu* unpairing line, then the dashed curve in the lower panel exhibits a point of inflection (while that in the middle panel has a robust minimum.)

D. Mixed Phase Alternatives

Up to this point, the phases we have discussed have been locally neutral with respect to all gauge charges. However, it is well known that neutrality can also be achieved in an averaged sense, by charge separation into a mixture of two oppositely charged phases. This is shown schematically in Fig. 9, which shows generic free energy curves $\Omega(\mu_i)$ for two phases A and B. The free energy must be a concave function of the chemical potential, since increasing μ_i increases the charge $Q_i = -\partial\Omega/\partial\mu_i$. There are then two possible situations. In one (Fig. 9b) there is no coexistence point and hence no mixed phase is possible. In the other (Fig. 9a) there is a coexistence point of oppositely-charged phases, and its free energy is lower than that of either neutral phase, so if Coulomb and surface energy costs are low enough then a neutral mixed phase will be free-energetically preferred over either homogeneous neutral phase.

We now consider possible gCFL+unpaired mixed phases. (Note that for $(M_s^2/\mu) > (M_s^2/\mu)_c$ a CFL+unpaired mixture is not possible because there is no CFL solution, charged or neutral.) For the unpaired and gCFL phases, the free energies are of the form shown in Fig. 9a. At the values of (μ_e, μ_3, μ_8) that make one phase neutral, the other phase has lower free energy. Thus there is a value of (μ_e, μ_3, μ_8) “between” that for

neutral gCFL and that for neutral unpaired quark matter, where the two can coexist with opposite color and electric charge density. However, a mixed phase is not favored in this case because each component would have net color charge, and color is a gauge symmetry with a strong coupling constant, so this mixed phase would pay a huge price in color-Coulomb energy. (For similar arguments applied to systems with no gauge symmetries, where the initial conclusion that a mixed phase is favored is the correct one, see Refs. [35, 36].)

It is then natural to ask whether one could construct a gCFL+unpaired mixed phase whose components are electrically charged, but color neutral. This avoids the large color-Coulomb energy cost of mixed phases with colored components. Such mixed phases have recently been constructed in two-flavor quark matter, with unpaired and 2SC components [37]. There is still some color electric field (and color-charged boundary layers) at the interfaces where the color chemical potentials change rapidly as one travels from one component to the other, analogous to the charged boundary layers and ordinary electric field at the CFL/nuclear interface constructed in Ref. [38], but Ref. [37] finds that the 2SC + unpaired mixed phase does occur in two-flavor quark matter. However, for color neutral unpaired and gCFL phases, we have found that the situation is typically that of Fig. 9(b): the free energy of color neutral, but electrically charged, unpaired quark matter is typically *higher* than the free energy of color-neutral gCFL, at the value of μ_e where color-neutral gCFL is electrically neutral. Hence there is no value of μ_e at which oppositely charged phases can coexist. We have found that this is true for all values of M_s^2/μ except for a range of a few MeV just below $M_s^2/\mu = 130$ MeV, where the neutral gCFL and neutral unpaired free energies cross. There, a mixed phase may arise, although as we shall discuss below it may be superseded by other more favorable possibilities.

We have not eliminated all possible mixed phase constructions, involving mixtures of all possible phases. However, over most of the gCFL regime there can be no mixed phase constructed from gCFL and unpaired quark matter.

E. (Gapless) 2SC and 2SCus

In this subsection, we discuss the properties of phases in which only two of the three flavors pair. These cannot compete with the CFL and gCFL phases at low values of M_s^2/μ , but could conceivably become important at larger values (lower densities).

The Fermi momenta in cold unpaired quark matter are ordered $p_{Fd} > p_{Fu} > p_{Fs}$, since the strange quark mass tends to decrease the strange quark Fermi momentum, and the down quark Fermi momentum then increases to preserve neutrality. Thus, the likely two-flavor pairings in cold three-flavor quark matter are u - d pairing (i.e. 2SC, with gap parameter $\Delta_3 > 0$ and $\Delta_1 = \Delta_2 = 0$) and u -

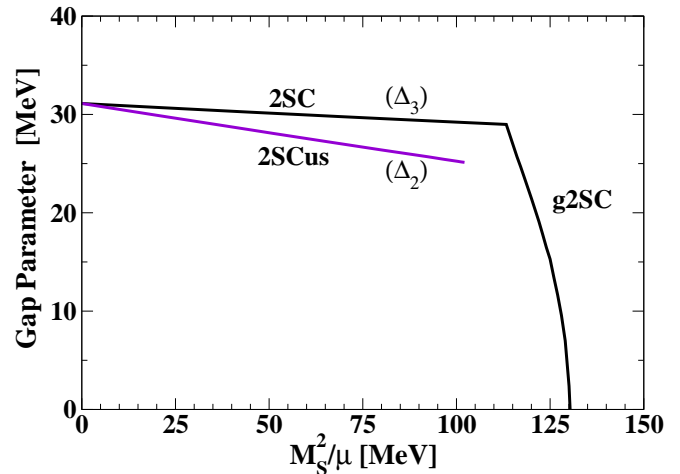


FIG. 10: Gap parameters in 3-flavor quark matter for the 2SC phase (Δ_3) and the 2SCus phase (Δ_2). In each case the other two gaps are zero. The 2SC phase becomes gapless (g2SC) at $M_s^2/\mu > 113$ MeV and ceases to exist at $M_s^2/\mu \approx 130$ MeV, and its free energy is always lower than that of unpaired quark matter (Fig. 3). The 2SCus phase becomes unfavored relative to unpaired quark matter at $M_s^2/\mu > 99$ MeV, and ceases to exist at $M_s^2/\mu \approx 103$ MeV, without ever becoming gapless.

s pairing (i.e. 2SCus, with gap parameter $\Delta_2 > 0$ and $\Delta_1 = \Delta_3 = 0$).

1. Calculation

In order to find a two-flavor pairing solution, we need only solve four equations (one gap and the three neutrality equations). The other two gap equations are automatically satisfied upon setting the relevant gaps to zero. Using the same coupling strength as in our investigation of the gCFL phase ($\Delta_0 = 25$ MeV) and working at the same value of $\mu = 500$ MeV, the nonzero gaps at $M_s^2/\mu = 0$ are $\Delta_3 = 31$ MeV in the 2SC phase and $\Delta_2 = 31$ MeV in the 2SCus phase. As we increase M_s^2/μ , as long as we do not enter a gapless phase the gaps decrease slowly and the simplified analysis of the 2SC and 2SCus phases in Ref. [8] should be a good guide. We do indeed find that our results are well approximated by $\mu_3 = \mu_8 = 0$ and $\mu_e = M_s^2/2\mu$ in the 2SC phase and $\mu_e = \mu_3 = \mu_8 = 0$ in the 2SCus phase, with a free energy given by

$$\Omega_{\text{neutral}}^{\text{2SC/2SCus}} = \Omega_{\text{neutral}}^{\text{unpaired}} + \frac{M_s^4 - 16\Delta_i^2\mu^2}{16\pi^2}, \quad (36)$$

with Δ_i given by Δ_3 in the 2SC phase and Δ_2 in the 2SCus phase, as predicted in Ref. [8]. The free energy of the 2SCus phase is higher than that of the 2SC phase because Δ_2 decreases more rapidly with M_s^2/μ in the 2SCus phase than Δ_3 does in the 2SC phase. This cannot be discovered by the methods of Ref. [8], in which these two phases were treated as degenerate.

Our results for the gap parameters are shown in Fig. 10 and for the free energies in Fig. 3. As in our other figures, we vary M_s keeping μ fixed at 500 MeV.

2. 2SC/g2SC Results

We find a neutral 2SC solution at low M_s^2/μ , with four gapped quasiparticles. At $M_s^2/\mu \approx 113$ MeV two of these quasiparticles become gapless, with blocking regions within which there are unpaired rd and gd quarks, and there is a continuous transition to the gapless 2SC (g2SC) phase. (Gapless 2SC was introduced in two-flavor quark matter in Refs. [21, 22].) The gap parameter then decreases rapidly until it reaches zero at $M_s^2/\mu \approx 130$ MeV and the solution ceases to exist.

As is clear from Fig. 3, 2SC/g2SC always has lower free energy than unpaired quark matter, and usually has higher free energy than CFL/gCFL. However, we find a tiny window of M_s^2/μ less than 1 MeV wide, very close to 130 MeV, in which the gapless 2SC phase has lower free energy than gCFL. In this regime, the one nonzero gap in the g2SC phase is almost zero whereas all three gaps are nonzero in the gCFL phase. This indicates that the fact that the gCFL free energy crosses that of unpaired quark matter almost at the same point where the g2SC and unpaired free energies come together is a non-generic feature of our model. Taken literally, our calculation predicts that as M_s^2/μ increases, gCFL is supplanted by g2SC which is then almost immediately supplanted by unpaired quark matter. However, treating the effects of M_s more accurately than we have may shut the tiny g2SC window completely [27]. In contrast, treating M_s as a chemical potential shift, as we have, but using $\Delta_0 = 100$ MeV appears to open a wide g2SC window [9], but this occurs in a regime where $M_s \sim \mu$ and so this result is not trustworthy. Also, as we discuss in the next section, a more general ansatz is required once one is at a sufficiently large M_s^2/μ that the free energy of the gCFL phase is close to that of unpaired quark matter, since there are other possible pairing patterns that likely become favorable.

Finally, it is interesting to note that the 2SC solution in three-flavor quark matter differs from its two-flavor version, which requires a large μ_e for neutrality given that there are no strange quarks present to carry negative charge. In three-flavor quark matter, we find that at $M_s = 0$ there is a small positive μ_e and a small negative $\mu_8 = -\mu_e$ in the 2SC phase. This happens because the pairing of ru , rd , gu and gd quarks increases their number density. This contributes a positive electric charge and excess redness/greenness, which is compensated by a small positive μ_e and a negative μ_8 . As we increase M_s^2/μ , the small μ_8 remains approximately unaffected whereas the small μ_e due to pairing is rapidly swamped by the larger contribution of order $M_s^2/2\mu$ that compensates for the lack of strange quarks.

3. 2SCus results

We find a neutral 2SCus solution, with a gap Δ_2 that decreases with increasing M_s^2/μ as shown in Fig. 10. This solution only exists for $M_s^2/\mu < 103$ MeV, and has a higher free energy than that of neutral unpaired quark matter for $M_s^2/\mu > 99$ MeV (see Fig. 3). It is always unfavored relative to the CFL/gCFL phase.

It is striking that two-flavor u - s pairing, unlike the two-flavor u - d pairing discussed above, has no gapless phase. In our calculations, we find that at $M_s^2/\mu > 103$ MeV, when the 2SCus phase becomes unstable to unpairing (i.e. when $\delta\mu_{\text{eff}}$ in the u - s sector, line 2 of table I, becomes as large as Δ_2), there is no neutral solution with a smaller value of Δ_2 (other than unpaired quark matter). We do find such a “gapless 2SCus” solution in a range of M_s^2/μ below 103 MeV, with Δ_2 smaller than that in the 2SC solution at the same M_s^2/μ , but the g2SCus solution is unstable: it is a local maximum of the neutral free energy as a function of Δ_2 . (In a figure like Fig. 7 this g2SCus solution would be at a local maximum of the *solid* curve.) At $M_s^2/\mu = 103$ MeV, the g2SCus solution (local maximum) meets the 2SCus solution (local minimum) at an inflection point of the neutral free energy, and for $M_s^2/\mu > 103$ MeV neither 2SCus nor g2SCus solutions exist. Unlike the gapless 2SC phase [21, 22] and the gapless CFL phase [6], which are rendered stable by the constraint of neutrality, the gapless 2SCus phase remains unstable. This is presumably because u - s paired phases are very close to being neutral anyway (only very small values of μ_e, μ_3, μ_8 are required to achieve neutrality [8]), so the constraint does not change the physics much. This can be summarized by saying that the 2SCus phase behaves analogously to that studied by Sarma [32], even after neutrality constraints are imposed.

IV. CONCLUDING REMARKS AND OPEN QUESTIONS

The gapless CFL phase seems sufficiently well-motivated as a possible component of compact stars to warrant further study of its low energy properties and its phenomenological consequences: it is the phase that supplants the asymptotic CFL phase as a function of decreasing density, and compact stars are certainly far from asymptotically dense.

The low energy effective theory of the gCFL phase must incorporate the gapless fermionic quasiparticles with quadratic dispersion relations, which have number densities $\sim \mu^2 \sqrt{\Delta_2 T}$ and dominate the low temperature specific heat, the gapless quarks with linear dispersion relations, with number densities $\sim \mu^2 T$, and the electron excitations, with number density $\sim \mu_e^2 T$. In contrast, the (pseudo-)Goldstone bosons present in both the CFL and gCFL phases have number densities at most $\sim T^3$. This means the gCFL phase will have very different phenomenology from CFL. It will be particularly

interesting to compute the cooling of a compact star with a gCFL core, because neutrino emission will require conversion between quasiparticles with linear and quadratic dispersion relations. And, we expect that in a star with CFL, gCFL and nuclear volume fractions, the gCFL shell will dominate the total heat capacity and the total neutrino emissivity, and thus control the (rapid) cooling. It will also be interesting to work out the magnetic field response of the gCFL phase, since the gauge boson propagators will be affected both by the gapless quasiparticles (all nine gauge bosons) and by the condensate (Meissner effect for eight out of nine.) Finally, we have left the study of possible meson condensation in the gapless CFL phase to future work.

Although we have studied the gCFL phase in a model, all of the qualitative properties of this phase that we have focussed on appear robust. We have also offered a model-independent argument for the instability that causes the transition, and for the location of the transition. We have used our model to show that the gCFL phase is favored over the two-flavor-pairing phases (2SC, g2SC, and 2SCus) throughout almost all of the regime where the gCFL phase is favored over unpaired quark matter. It remains a possibility, however, that the CFL gap is large enough that baryonic matter supplants the CFL phase before $M_s^2/\mu > 2\Delta$. Assuming that the gCFL phase does replace the CFL phase, it is also possible that gaps are small enough that a third phase of quark matter could supplant the gCFL phase at still lower density, before the transition to baryonic matter. We do not trust our analysis to determine this third phase. Perhaps it is a mixed phase of some sort, although we have ruled out the straightforward possibilities. Perhaps it is the gapless 2SC phase [21, 22], as the literal application of our model would suggest. We should stress, in addition, that our model relies upon a pairing ansatz designed to study the instability of the CFL phase, and hence well-suited to the study of the gCFL phase. Determining what phase comes after gCFL almost certainly requires a more general ansatz. For example, perhaps weak pairing between quarks with the same flavor plays a role once gCFL is superseded [39], or perhaps it is the crystalline color superconducting phase [26, 29, 30, 40, 41] that takes over from gapless CFL at lower densities. (Other possibilities have also been suggested [42].)

Recent developments [41] make the crystalline color superconducting phase look like the most viable contender for the “third-from-densest phase”. Previous work [40] had suggested that the face-centered-cubic crystal structure was sufficiently favorable that its free energy could be competitive with that of BCS pairing over a wide range of parameter space, but because these indications came from a Ginzburg-Landau calculation pushed beyond its regime of validity, quantitative results were not possible. The results of Ref. [41] suggest that a crystalline phase involving pairing of only two flavors is favored over the unpaired phase by $\approx 0.2\mu^2\Delta_{2SC}^2/\pi^2$ at $M_s^2/\mu \approx 4\Delta_{2SC}$. Here, Δ_{2SC} is the gap parameter in the 2SC phase at $M_s = 0$, which is 31 MeV with the parameter values we have used in all our figures. This suggests that if we were to generalize our pairing ansatz to allow the crystalline phase as a possibility, it would take over from gCFL at $M_s^2/\mu \sim 120$ MeV, or even somewhat lower if the three-flavor crystalline phase, which no one has yet constructed, is more favorable than the two-flavor version. Furthermore, the authors of Ref. [41] find that the crystalline phase persists until a first order crystalline \rightarrow unpaired transition at $M_s^2/\mu \approx 7.5\Delta_{2SC}$, hence over a very wide range of densities. If analysis of three-flavor crystalline color superconductivity supports these estimates, we will not have to worry about the resolution of the puzzles and possible mixed phases associated with the confluence of the free energies for the gCFL, g2SC and unpaired phases near $M_s^2/\mu \sim 130$ MeV in Fig. 3: by that density the crystalline phase will already be robustly ensconced on the phase diagram.

Acknowledgments

We acknowledge helpful conversations with J. Bowers, R. Casalbuoni, G. Cowan, M. Forbes, K. Fukushima, E. Gubankova, J. Kundu, W. V. Liu, G. Nardulli, S. Reddy, T. Schäfer, I. Shovkovy and F. Wilczek, and are grateful to the INT at the University of Washington in Seattle for its hospitality. This research was supported in part by DOE grants DE-FG02-91ER40628 and DF-FC02-94ER40818.

-
- [1] For reviews, see K. Rajagopal and F. Wilczek, arXiv:hep-ph/0011333; M. G. Alford, Ann. Rev. Nucl. Part. Sci. **51**, 131 (2001) [arXiv:hep-ph/0102047]; G. Nardulli, Riv. Nuovo Cim. **25N3**, 1 (2002) [arXiv:hep-ph/0202037]; S. Reddy, Acta Phys. Polon. B **33**, 4101 (2002) [arXiv:nucl-th/0211045]; T. Schäfer, arXiv:hep-ph/0304281.
- [2] Conceptual Design Report “An International Accelerator Facility for Beams of Ions and Antiprotons”, GSI Darmstadt, 2001, <http://www.gsi.de/GSI-Future/cdr/>.
- [3] M. Kitazawa, T. Koide, T. Kunihiro and Y. Nemoto, Phys. Rev. D **65**, 091504 (2002) [arXiv:nucl-th/0111022]; D. N. Voskresensky, arXiv:nucl-th/0306077.
- [4] M. G. Alford, K. Rajagopal and F. Wilczek, Nucl. Phys. B **537**, 443 (1999) [arXiv:hep-ph/9804403].
- [5] M. Gyulassy and L. McLerran, arXiv:nucl-th/0405013; E. V. Shuryak, arXiv:hep-ph/0405066.
- [6] M. Alford, C. Kouvaris and K. Rajagopal, Phys. Rev. Lett. **92** 222001 (2004) [arXiv:hep-ph/0311286].
- [7] K. Iida and G. Baym, Phys. Rev. D **63**, 074018 (2001)

- [hep-ph/0011229].
- [8] M. Alford and K. Rajagopal, *JHEP* **0206**, 031 (2002) [arXiv:hep-ph/0204001].
- [9] S. B. Ruester, I. A. Shovkovy and D. H. Rischke, arXiv:hep-ph/0405170.
- [10] M. G. Alford, J. Berges and K. Rajagopal, *Nucl. Phys. B* **571**, 269 (2000) [arXiv:hep-ph/9910254].
- [11] D. K. Hong, *Nucl. Phys. B* **582**, 451 (2000) [arXiv:hep-ph/9905523]; N. J. Evans, J. Hormuzdiar, S. D. H. Hsu and M. Schwetz, *Nucl. Phys. B* **581**, 391 (2000) [arXiv:hep-ph/9910313].
- [12] D. T. Son and M. A. Stephanov, *Phys. Rev. D* **61**, 074012 (2000) [arXiv:hep-ph/9910491]; *Phys. Rev. D* **62**, 059902 (2000) [arXiv:hep-ph/0004095]. D. K. Hong, T. Lee and D. P. Min, *Phys. Lett. B* **477**, 137 (2000) [arXiv:hep-ph/9912531]; C. Manuel and M. H. G. Tytgat, *Phys. Lett. B* **479**, 190 (2000) [arXiv:hep-ph/0001095]; S. R. Beane, P. F. Bedaque and M. J. Savage, *Phys. Lett. B* **483**, 131 (2000) [arXiv:hep-ph/0002209]; T. Schafer, *Phys. Rev. D* **65**, 074006 (2002) [arXiv:hep-ph/0109052].
- [13] P. F. Bedaque and T. Schafer, *Nucl. Phys. A* **697**, 802 (2002) [arXiv:hep-ph/0105150]; D. B. Kaplan and S. Reddy, *Phys. Rev. D* **65**, 054042 (2002) [arXiv:hep-ph/0107265]; A. Kryjevski, D. B. Kaplan and T. Schafer, arXiv:hep-ph/0404290.
- [14] J. Madsen, *Phys. Rev. Lett.* **85**, 10 (2000) [arXiv:astro-ph/9912418]; C. Manuel, A. Dobado and F. J. Llanes-Estrada, arXiv:hep-ph/0406058.
- [15] S. Reddy, M. Sadzikowski and M. Tachibana, *Nucl. Phys. A* **714**, 337 (2003) [arXiv:nucl-th/0203011]; P. Jaikumar, M. Prakash and T. Schafer, *Phys. Rev. D* **66**, 063003 (2002) [arXiv:astro-ph/0203088]; J. Kundu and S. Reddy, arXiv:nucl-th/0405055; I. A. Shovkovy and P. J. Ellis, *Phys. Rev. C* **66**, 015802 (2002) [arXiv:hep-ph/0204132].
- [16] M. G. Alford, J. Berges and K. Rajagopal, *Nucl. Phys. B* **558**, 219 (1999) [arXiv:hep-ph/9903502].
- [17] T. Schafer and F. Wilczek, *Phys. Rev. D* **60**, 074014 (1999) [arXiv:hep-ph/9903503].
- [18] M. Buballa and M. Oertel, *Nucl. Phys. A* **703**, 770 (2002).
- [19] A. W. Steiner, S. Reddy and M. Prakash, *Phys. Rev. D* **66**, 094007 (2002) [arXiv:hep-ph/0205201].
- [20] F. Neumann, M. Buballa and M. Oertel, *Nucl. Phys. A* **714**, 481 (2003) [arXiv:hep-ph/0210078].
- [21] I. Shovkovy and M. Huang, *Phys. Lett. B* **564**, 205 (2003);
- [22] M. Huang and I. Shovkovy, arXiv:hep-ph/0307273.
- [23] P. Amore, M. C. Birse, J. A. McGovern and N. R. Walet, *Phys. Rev. D* **65**, 074005 (2002) [arXiv:hep-ph/0110267].
- [24] A. Gerhold and A. Rebhan, *Phys. Rev. D* **68**, 011502 (2003) [arXiv:hep-ph/0305108]; A. Kryjevski, *Phys. Rev. D* **68**, 074008 (2003) [arXiv:hep-ph/0305173]; D. D. Dietrich and D. H. Rischke, *Prog. Part. Nucl. Phys.* **53**, 305 (2004) [arXiv:nucl-th/0312044].
- [25] K. Rajagopal and F. Wilczek, *Phys. Rev. Lett.* **86**, 3492 (2001) [arXiv:hep-ph/0012039].
- [26] J. Kundu and K. Rajagopal, *Phys. Rev. D* **65**, 094022 (2002) [arXiv:hep-ph/0112206].
- [27] We have learned in private communication from K. Fukushima that treating the effects of M_s in full, rather than as a shift in the strange quark effective chemical potential, changes our results by only a few percent, for the choices of Δ_0 and M_s at which we quote results.
- [28] W. V. Liu, F. Wilczek and P. Zoller, arXiv:cond-mat/0404478.
- [29] P. Fulde and R. A. Ferrell, *Phys. Rev.* **135**, A550 (1964); S. Takada and T. Izuyama, *Prog. Theor. Phys.* **41**, 635 (1969); M. G. Alford, J. A. Bowers and K. Rajagopal, *Phys. Rev. D* **63**, 074016 (2001) [arXiv:hep-ph/0008208]; R. Casalbuoni and G. Nardulli, *Rev. Mod. Phys.* **263**, 320 (2004) [arXiv:hep-ph/0305069].
- [30] J. A. Bowers, J. Kundu, K. Rajagopal and E. Shuster, *Phys. Rev. D* **64**, 014024 (2001) [arXiv:hep-ph/0101067].
- [31] E. Gubankova, W. V. Liu and F. Wilczek, *Phys. Rev. Lett.* **91**, 032001 (2003).
- [32] G. Sarma, *J. Phys. Chem. Solids* **24**, 1029 (1963);
- [33] M. G. Alford, J. Berges and K. Rajagopal, *Phys. Rev. Lett.* **84**, 598 (2000) [arXiv:hep-ph/9908235].
- [34] W. V. Liu and F. Wilczek, *Phys. Rev. Lett.* **90**, 047002 (2003) [arXiv:cond-mat/0208052].
- [35] P. F. Bedaque, H. Caldas and G. Rupak, *Phys. Rev. Lett.* **91**, 247002 (2003) [arXiv:cond-mat/0306694].
- [36] M. M. Forbes, E. Gubankova, W. V. Liu and F. Wilczek, arXiv:hep-ph/0405059.
- [37] S. Reddy and G. Rupak, arXiv:nucl-th/0405054.
- [38] M. G. Alford, K. Rajagopal, S. Reddy and F. Wilczek, *Phys. Rev. D* **64**, 074017 (2001) [arXiv:hep-ph/0105009].
- [39] M. Iwasaki and T. Iwado, *Phys. Lett. B* **350**, 163 (1995); M. G. Alford, K. Rajagopal and F. Wilczek, *Phys. Lett. B* **422**, 247 (1998) [arXiv:hep-ph/9711395]; T. Schafer, *Phys. Rev. D* **62**, 094007 (2000) [arXiv:hep-ph/0006034]; M. Buballa, J. Hosek and M. Oertel, *Phys. Rev. Lett.* **90**, 182002 (2003) [arXiv:hep-ph/0204275]; A. Schmitt, Q. Wang and D. H. Rischke, *Phys. Rev. D* **66**, 114010 (2002) [arXiv:nucl-th/0209050]; M. G. Alford, J. A. Bowers, J. M. Cheyne and G. A. Cowan, *Phys. Rev. D* **67**, 054018 (2003) [arXiv:hep-ph/0210106]; A. Schmitt, arXiv:nucl-th/0405076.
- [40] J. A. Bowers and K. Rajagopal, *Phys. Rev. D* **66**, 065002 (2002) [arXiv:hep-ph/0204079].
- [41] R. Casalbuoni, M. Ciminale, M. Mannarelli, G. Nardulli, M. Ruggieri and R. Gatto, arXiv:hep-ph/0404090.
- [42] H. Muther and A. Sedrakian, *Phys. Rev. D* **67**, 085024 (2003) [arXiv:hep-ph/0212317]; A. Iwazaki and O. Morimatsu, *Phys. Lett. B* **571**, 61 (2003) [arXiv:nucl-th/0304005].